JMEPEG (2022) 31:6131–6148
https://doi.org/10.1007/s11665-022-07149-w

1059-9495/$19.00

REVIEW

Laser Additive Manufacturing of Titanium-Based Functionally Graded Materials: A Review

Shivank A. Tyagi and M. Manjaiah

Submitted: 11 September 2021 / Revised: 1 July 2022 / Accepted: 6 July 2022 / Published online: 22 July 2022

Functionally graded materials (FGMs) refer to advanced engineering materials that exhibit exceptional thermo-mechanical characteristics due to their intrinsic spatial variation in properties across the volume. These materials provide an elegant solution for the cases where the parts are subjected to varying thermal or mechanical loads over a region of interest. For this reason, FGMs have found their applications in areas including aerospace, defense, mining and naval manufacturing sectors. Particularly in the aerospace industry, the properties of FGMs have been harnessed to develop heat-resistant surfaces for the space shuttle and aircraft engine components. One of the most relevant methods in the production of FGMs is the use of additive manufacturing (AM) techniques. Especially directed energy deposition (DED) method is one of the leading technologies to produce physical objects from the 3D CAD model. Titanium and nickel are one of the most efficient materials used in aerospace. Several studies have been carried out to develop suitable Ti- and Ni-based alloys and composites for specific applications. Moreover, several researchers have developed FGMs based on Ti or its alloys with materials like Al, Ni, Mo, Nb, etc. The current article presents a state of art conceptual understanding of additively manufactured FGMs, covering an overview of the DED technique and effects of the process parameters involved that can enable the manufacturing of FGM parts. The limitations of certain AM technologies are briefly discussed. In addition, possible strategies to overcome the challenges and future opportunities of AM technology to fabricate Ti-based FGMs and structures were presented.

Keywords additive manufacturing, direct energy deposition, FGMS, properties of fabrication, Ti and Ni alloys

1. Introduction

Functionally graded materials (FGMs) are a group of advanced engineering materials which exhibit gradual variation in their chemical composition and structure throughout the volume. These are a representative example of property tailored components. In FGMs the properties of the final component are a function of position which is a result of controlled changes in composition or microstructures achieved with the help of specific manufacturing techniques. The inspiration for FGMs came from some of the naturally occurring materials like wood, bone, teeth, bamboo, etc. (Ref 1, 2, 3), and the initial industrial application of FGMs dates back to 1980's in Japan where the driving force for the development of FGMs was the challenge of designing a thermal barrier coating on surface of the space planes or re-entry space vehicles capable of withstanding a temperature of about 1500-1800 °C (Ref 4).

Over the years, several manufacturing techniques have been adopted for the development of FGMs. Some of the recent trends involve the use of powder metallurgy for the production of FGMs (Ref 5, 6). Powder metallurgy can be used to manufacture FGMs with simple shape and size. Further, secondary operations may be required for the elimination of porosity from the fabricated part. Certain applications require the production of cylindrical components with functionally graded property variation. In such cases centrifugal casting technique is employed (Ref 7). In this method, there is a limit on the type of gradient that can be produced as the development of gradient solely depends on the difference in the centrifugal force produced due to variation in density between solid particles and molten metal (Ref 8, 9). Apart from the discussed bulk processing techniques, functionally graded surface coatings have been extensively used to provide excellent surface protection to the parts against high temperatures, wear, corrosion and oxidation. For example, functionally graded coatings of alumina-SiC over 316L stainless steel are preferred for thermal barrier coatings (TBC), environmental barrier coatings (EBC) and biomaterials (Ref 10). Several vapor deposition techniques like sputter deposition, chemical vapor deposition (CVD) and physical vapor deposition (PVD), plasma enhanced chemical vapor deposition, etc., are in use for developing functionally graded surface coatings (Ref 11, 12). However, these processes have certain disadvantages as they are energy intensive and produce poisonous gases (Ref 13).

This invited article is part of a special issue in the *Journal of Materials Engineering and Performance* entitled "Space and Aerospace Exploration Revolution: Metal Additive Manufacturing." The issue was organized by Shahrooz Nafisi, Relativity Space; Paul Gradl, NASA Marshall Space Flight Center; Douglas Hofmann, NASA Jet Propulsion Laboratory/California Institute of Technology; and Reza Ghomashchi, The University of Adelaide, Australia.

Shivank A. Tyagi and **M. Manjaiah**, Department of Mechanical Engineering, National Institute of Technology, Warangal, Telangana 506004, India. Contact e-mail: manjaiah.m@nitw.ac.in.

Studies show that a wide range of materials can be used for developing parts with functional gradation in properties by employing different techniques as discussed earlier. C/SiC FGM was developed using CVD process by Kawase et al. (Ref 14) and also material combinations like WC/Co/diamond were used to develop FGM with high wear resistance and toughness using chemical vapor infiltration (CVI) (Ref 15). Moreover, a significant variety of FGMs (ZrB_2-SiC/ZrO_2 (Ref 16), Al_2O_3-Ti_3SiC_2 (Ref 17), W-Cu (Ref 18) and SiC-Al_3BC_3 (Ref 19)) were manufactured using spark plasma sintering (SPS) with an aim to obtain good mechanical characteristics. Rajan et al. (Ref 20) developed high hardness Al-SiCp functionally graded metal matrix (FGMM) composites using centrifugal casting. Apart from these, FGM systems like Ti-TiB_2 (Ref 21) and Ti-TiB (Ref 22) were successfully prepared by powder metallurgy (PM) technique.

Of all the materials discussed above and many more that have been studied. Titanium is one of the important engineering material and it has found major applications in biomedical field (implants, scaffolds, bone plated, etc.), aerospace (airframe and the engine parts (Ref 2), space launch vehicle (Ref 1)) and automobile industry (Ref 23). This is due to its high strength to weight ratio, good thermal and corrosion resistance. For this reason, manufacturing of Ti-based FGMs has been a matter of research for several years. Some of the methods used for manufacturing of Ti-based FGMs are summarized in Table 1.

Even though these studies show successful implementation of the methods mentioned in Table 1 and are still in use, they have certain limitations like production of toxic waste and (chemical solution deposition), manufacturing is restricted to simple shapes (selective plasma sintering, powder metallurgy), and for powder metallurgy the process is economical only for mass production. In case of reaction sintering, the components react together during sintering process; hence, the materials that can be used become limited. This is also the case with SCS where a wave of chemical reactions traveling layer by layer leading to combustion of compacted powder is utilized for manufacturing of desired FGMs. As the accurate control over chemical reactions is difficult to achieve, the accuracy in obtaining desired property gradation reduces in such methods. However, these methods can still be used based on how closely they fulfill requirements of a particular application (Table 2).

One of the recent developments in production of FGMs is the use of additive manufacturing (AM) techniques that can account for some of the limitations of conventional methods. It is one of the leading technologies where physical objects can be produced directly from the computer-generated data of the component. Remarkable results have been obtained due to its ability to control internal geometrical features of the part, a significant reduction in overall product development and manufacturing time, ability to produce near net shape components, maximum material utilization and ability to fabricate complex shapes and designs (Ref 30). Among several AM techniques, laser-based methods are most commonly used for production of FGMs. These include methods like powder bed fusion (PBF) (Ref 31) and directed energy deposition (DED) (Ref 30). However, for laser powder bed fusion (L-PBF)-based method, it is not feasible to obtain compositional or constitutional gradients along different directions. This is not the case with DED techniques like laser powder DED (LP-DED) where the layer is developed by point-to-point deposition as different powders with different feed rates can be directed towards a point followed by melting using laser heating and rapid solidification (Ref 31).

2. Direct Energy Deposition (DED) Process

Directed energy deposition (DED) is an additive manufacturing technique that utilizes a concentrated source of heat (laser, electron beam, electric arc), with in situ supply of powder or wire shaped material for subsequent melting to achieve layer-by-layer part fabrication or single-to-multi layer cladding/repair. Three processes currently can be categorized under this type: the laser powder directed energy deposition (LP-DED), the electron beam freeform fabrication (EBFF) and the wire and arc additive manufacturing (WAAM) (Ref 32). These methods are extensively used for development of near net-shaped components.

Laser-based direct energy deposition (LP-DED and LW-DED) has been investigated thoroughly in the past years as it provides several advantages such as (i) rapid prototyping of metallic parts, (ii) fabrication of customized and complex parts, (iii) clad/repair valuable metallic parts and (iv) manufacture/repair in logistically intricate locations.

Some of the initial developments of additive manufacturing involving simultaneous delivery of energy/material, including modern DED, comes from ‘welding AM’ era-as indicated by the patents of Harter and Kratky (Ref 34, 35). With the advancement of private industry, Brown et al. further extended the concepts of DED in a patent that described layer-wise, additive deposition via combined laser/powder (or wire) metallurgy (Ref 36). Through the 1980s there was little development in DED-based technology. Later on, Mehta et al. (Ref 37) patented a method to repair metallic articles via combined application of a laser and blown powder with a specific focus on delivering a consistent, continuous flow of powder for the subsequent melting. Further in 1990s, German-based direct laser deposition (DLD) technique called ‘Controlled metal build up’ was successfully implemented (Ref 38, 39). In order to improve the efficiency of the technique, Hammeke (Ref 40) and Buongiorno (Ref 41) developed a combined laser/powder delivery mechanisms (e.g., deposition heads).

Laser-based DED employs metals and alloys in powder or wire form that are directly deposited to a substrate coupled with simultaneous irradiation of a laser beam, accompanied by the moving substrate. The use of powder results in lower deposition efficiency while wire fed DED process can yield 90% efficiency (Ref 42). It may be due to the fact that only a fraction of the total powder melts and bonds to the substrate. Also, powder usage leads to higher complexity and resolution of parts to be fabricated, whereas the wire fed method is suitable for producing large size components due to higher deposition rates (Ref 43, 44). Powder DED and wire DED both develops a pool of molten metal that travels in space/time efficiently creating a 3D part from zero medium as illustrated in Fig. 1. For LP-DED a focused laser beam coincides with the deposition head, which may comprise either a single or multiple powder-spray nozzles, whereas wire-DED utilizes an arc (electric or plasma) or laser beam (LW-DED) as heat energy and a wire feedstock (Ref 45). Typically for LP-DED, as particles are deposited, the laser beam delivers adequate thermal energy to melt the powder particles into the melt pool. However, in some advanced LP-

Table 1 Conventional methods used for developing Ti-based FGMs

S. no	Process used	FGM system	Description	Reference
1	Chemical solution deposition	Ti/HAP coatings on Ti-6Al-4V	Ti_{100-x}/HAP_x (x = 0 to 100%) films were developed over Ti-6Al-4V implants	(Ref 24)
2	Mixed-powder pouring method and spark plasma sintering (SPS)	ZrO_2 and Ti particles	Ti-ZrO_2 FGMs were fabricated, using different sizes of ZrO_2 and Ti particles	(Ref 25)
3	Powder metallurgy (PM)	Ti+HA	As the content of Hydroxyapatite increases, the Young's modulus and the compressive strength decrease	(Ref 26)
4	Spark plasma sintering	Al_2O_3-Ti and Al_2O_3-TiH_2 FGM	The combination of Al_2O_3 and Ti powders is suitable to fabricate the FGM	(Ref 27)
5	Reaction Sintering	Ti-TiB	In situ formation of TiB whiskers and densification due to reaction sintering was utilized for developing FGM	(Ref 28)
6	Simultaneous combustion synthesis (SCS)	TiC-Ni	SCS and hot compaction of Ti, C and Ni powders under a hydrostatic pressure was undertaken to fabricate fully dense TiC-Ni FGM	(Ref 29)

Table 2 Literature on additive manufacturing of Ti-based FGMs

S No	AM process	FGM system	Composition/grading ,vol.% or Wt.%	No of layers (Zones)	Mechanical characteristics		Study	Ref
					Tensile strength, MPa	Hardness		
1	LP-DED	Ti-6Al-4V /V	100 vol.% Ti64 to 100 Vol% V with 3% increment	195 layers with 35 individual compositions	828-776	47-2 HRC	A roadmap for fabricating FGMs that generally cannot be obtained using standard metallurgy techniques was provided	(Ref 97)
2	LP-DED	Ti-6Al-4V /V	100 wt.% Ti to Ti-25 wt.% V	13	…	205-420 VHN	Microstructure evolution in α/β Ti-V alloy FGM	(Ref 98)
3	EBM	TC4/TiAl	**Sample 1**-100 wt% TiAl to 0% in 2 increments **Sample 2**-0 wt% TiAl to 60% in 3 increments	Sample 1-20 Sample 2-50	…	Microhardness-350-450 Mpa	The chemical compositions, microstructure and micro-hardness of the dual material samples were investigated	(Ref 99)
4	LP-DED	Ti6Al4V/ AlSi10Mg	From 100 wt.% Ti6Al4V to 100 wt.% AlSi10Mg with an increment of 25%	5	417	214-619 HV	Effect of process parameters on microstructure, tensile and microhardness	(Ref 100)
5	LP-DED	Ti6Al4V/ Mo	0 to 100 wt.% Mo with 25 wt% increments	5	…	190-450 HV	Microstructure and micro-hardness analysis	(Ref 101)
6	LPBF	Ti-6Al-4V	34.11 and 26.62% gradient in elastic modulus and hardness, respectively was obtained	…	Up to 100 Mpa	Up to 4 GPa	Gradient in material defects (Ref pores, cracks) developed due to variation in process parameters was observed	(Ref 102)
7	LW-DED	Ti6Al4V/TiC_p	From 100 vol.% Ti64 alloy to 50 vol.% TiCp with an increment of 5%	51	820	375-730 HV	Effect of TiC_p addition on microstructure and mechanical properties	(Ref 103)
8	LP-DED	Ti-6Al-4V/ V/304L SS	**Composition 1:** 100 vol.% Ti64 to 75 vol.% V **Composition 2:** 25% SS/75% V to 50% SS/V	142	…	490 ± 48 to 713 ± 220 HV	Characterization of phase composition and properties	(Ref 104)
9	LP-DED	Ti6Al4V/ZrO_2	Compositions of 100% Ti6Al4V, 80% Ti6Al4V + 20%ZrO2, 60% Ti6Al4V + 40%ZrO2	28	…	390-790 HV	Mechanical, microstructure and wear analysis of FGM was studied	(Ref 105)

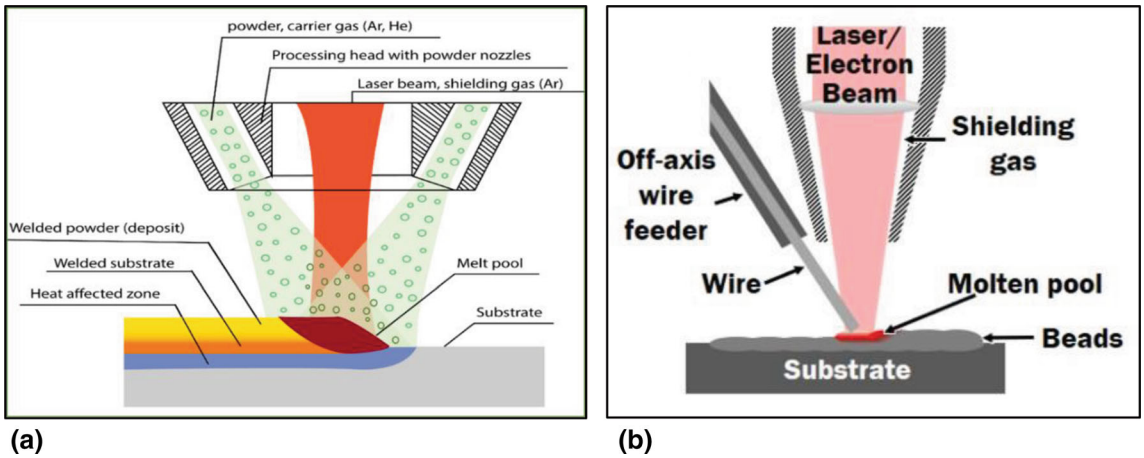

Fig. 1 (a) Powder fed direct energy deposition, (b) wire fed direct energy deposition (Ref 33). Figure2b by Dong-Gyu Ahn in *International Journal of Precision Engineering and Manufacturing-Green Technology,* Vol 7, Pages 703–742 is licensed under CC BY 4.0

DED process extreme high-speed laser material deposition (EHLD) technology is utilized where a focal region of fed powder is created to melt the powder before hitting the melt pool (Ref 46) along the deposition direction. Powder DED machines are often provided with supply of inert gas, together with the powder from the nozzles, thereby shielding the molten metal pool, reducing the rate of oxidization (Ref 33). This generates a molten metal pool and below it is a heat-affected zone (HAZ) with variable depth of penetration. Once the deposition of a single layer is complete, the build plate moves by means of CNC or CAD data with respect to the deposition head which moves in build direction and the process is repeated. Studies have shown that in certain situations wire-based DED method is beneficial for improved efficiency and good surface quality (Ref 47, 48). However, their applications in the domain are relatively less than powder-fed DED. This may be due to the fact that blown powder dynamics are easier to control in real-time as response lag is less and these can be tailored for more precise manufacturing of complex geometries. Also, recycling of powder makes it relatively economical. However, wire-fed DED is prone to instability in case of uneven deposition surfaces, excessive residual stress and deterioration and poor surface roughness (Ref 49, 50). LP-DED can be utilized for fabrication of a variety of metals and ceramics including: stainless steels, titanium alloy (Ti-Ni, Ti-Al, Ti-Nb, etc.), Inconel 625, H13 tool steel, chromium, tungsten and several other materials (Ref 51, 52).

With the ongoing technological advancements, a number of studies have been conducted to improve the efficiency of the process. Some recent developments in LP-DED research are focused on areas like optimization of process parameters (laser power, powder feed rate, scan speed, hatch spacing and layer thickness) in accordance with the material being dealt with. As the number of compatible materials increases, it is significant to select a suitable process window for desired results (Ref 53). It has been observed in LP-DED that there is a local variation in laser absorption due to factors like surface morphology, the effect of pre-heating, powder feed rate, etc. To counter this effect a real-time control of process parameters is required which was addressed by Sorn et al. (Ref 54). In situ imaging and temperature monitoring provide a means for examining imperfections like cracks, lack of fusion and analysis of geometry in LP-DED (Ref 55). Another advantage of having control over parameters is the ability of LP-DED process to conceive tailored mechanical and microstructural characteristics by adjusting cooling rate of the component (Ref 56). One of the recent developments in LP-DED is fabrication of smart components which include embedded sensors for remotely monitoring physical parameters like pressure, temperature, etc. It has applications like embedded optical fiber sensors in the cutting tool fabricated by combining LP-DED and molding. These sensors have smaller size, lightweight, good durability and external electromagnetic field immunity, etc. (Ref 57, 58).

The processing parameters (laser power, scan speed, powder feed, etc.) selected for fabrication of the components have a significant effect on the grain growth, microstructure and intermetallic phases, which greatly affect the final properties of the part. The following section briefly discusses the important aspects that must be taken care of in the selection of optimal process parameters.

3. Effect of Process Parameters

In LP-DED process as the laser beam is concentrated and a stream of powder material is fed, they intersect at a common point where the material melts due to the energy of laser beam and a melt pool is generated. In case of manufacturing of FGMs, when there are multiple materials to be alloyed over graded compositions layer by layer, the heat from previously solidified layers gets accumulated and can sometimes lead to re-melting of layers which may cause intermixing between layers of different compositions. However, as there is always substantial re-melting of the previous layers otherwise, there is possibility of getting lack of fusion defects. This limits the minimum re-melting possible which is usually quite high. The consequent dilution and mixing will affect the maximum functional composition gradient that can be obtained. But in some cases excessive remelting of layers may homogenize the composition to a certain degree in that region and hence negatively affect the graded composition (Ref 59). To overcome this, sometimes the laser power is gradually reduced in steps to prevent accumulation of excess heat. Inside the melt-pool, the surface tension and convection currents driven flow of molten metals can considerably affect the heat transfer,

segregation and porosity and depth of penetration of melt-pool (Ref 60). This flow may also lead to inter-mixing between the graded layers and 'dilution' from the substrate. Studies show that dilution (D) depends on several factors like, thermal conductivity & reflectivity of the material, initial temperature of the substrate, powder feed rate and laser power (Ref 61, 62). A mathematical relation for predicting dilution in LP-DED process is available Eq 1:

$$D = \left(1 + \frac{\eta_d v_p \Delta H_S}{\eta_a \eta_m P - \eta_a v_p \Delta H_p}\right)^{-1} \quad \text{(Eq 1)}$$

where, η_a, η_d and η_m are the efficiencies of energy transfer, deposition and melting and V_p, ΔH_p, ΔH_s and P are the volume of powder, melting enthalpy of powder, melting enthalpy of substrate and laser power, respectively. An optimum value of laser power is necessary to obtain adequate deposition. Higher laser power will result in higher dilution and for too high values it may even lead to vaporization of deposited material or plasma formation (Ref 63). It is seen that with increase in laser power the size of melt pool increases up to a certain limit beyond which further increase in power only raises the temperature of melt pool without changing its depth (Ref 64). Apart from laser power another important parameter in this regard is the scanning velocity. For too low value of scanning velocity the dilution will increase. Hence, the effects of laser power and scanning velocity are inversely proportional in laser metal deposition process. Another term representing relation between melted substrate and deposited powder is geometric dilution 'DG', it is evaluated by Eq 2.

$$\mathrm{DG} = \frac{A_s}{(A_p + A_s)} \quad \text{(Eq 2)}$$

where A_s is cross-sectional area of melted substrate and A_p is the cross-sectional area of deposited powder. Studies show that keeping laser power and powder feed rate constant, the geometric dilution increases with increasing scan speed and becomes constant at higher scan speeds (Ref 64). When the melt pool is small, for low powers the cooling rates of the liquid melt pool at the interface are higher. With the increase in laser power the cooling rates decreases and at peak power, as the bulk heating of the substrate occurs away from the melt zone, the cooling rates may drop to even lower values leading to a coarsened microstructure due to grain growth. These processes can be modelled using finite element techniques (Ref 65). Also, if temperature gradients (ΔT) developed between the graded layers and intermetallic phases exceeds a certain limit it can lead to generation of internal stresses which can cause cracking. It is known that cracking may occur in the deposited structure if the residual internal stresses go beyond the yield strength of the material (Ref 66, 67). Based on the studies of Chen et al. (2017) (Ref 68) and Meng et al. (2020) (Ref 69), for a gradient structure deposited by LP-DED the internal stress developing in build direction between layers due to inconsistency in expansion and contraction can be calculated using Eq 3:

$$\sigma = \frac{E \Delta\alpha \Delta T}{1 - \mu} \quad \text{(Eq 3)}$$

where σ is the internal stress, $\Delta\alpha$ is the difference of the coefficient of thermal expansion (CTE) between the layers, E is Young's modulus of a deposited gradient material layer (Ref 70), ΔT is the temperature gradient between the center and surface of the melt pool and μ is the Poisson's ratio.

Another important aspect of the DED process is the accuracy with which desired gradient composition is attained in the final part. In order to achieve this, at different layers, it is imperative to have a precise powder feeding setup (Ref 71). With recent developments in fabrication of FGMs the focus is not only on developing gradients (compositional, microstructural) along the build direction, but also across the build (i.e., developing gradient across a single deposited track). Whereas, for producing gradients along the height of the part continuous coaxial nozzles are used, in case of developing gradients along a single deposited track, discrete coaxial nozzles are more efficient (Ref 72). The above discussion helps to understand how different processing conditions in additive manufacturing can affect the final properties of a part (FGMs in present context) and also how these concepts relate to the causes of defects like porosity, development of excessive residual stresses between consecutive layers in case of FGMs, distortion, cracking, lack of fusion, undesired compositional gradients, etc.

4. Additive Manufacturing of Ti-Based Functionally Graded Materials

Functionally graded materials provide an opportunity to obtain tailored mechanical and thermal properties by controlling the variations in microstructure and composition across the bulk of material (Ref 73). As discussed earlier, Ti is an attractive engineering material by virtue of its high strength to weight ratio, good resistance to corrosion and high temperature bearing characteristics (Ref 74, 75). Some of the major applications involve use of Ti in airframes, rocket engines, gas turbine engines (Ref 76) and thermal protection in hypersonic airplanes (Ref 77). Also Ti is an important structural material for developing space launch vehicles (Ref 1).

Few researchers have developed FGMs based on Ti or its alloys with materials like Al, Ni alloys (Inconel 625, Inconel 718, Monel), Mo, Nb, steel, etc. Due to cost effectiveness of Al, Ti-Al-based structures are popular in aerospace and automobile industries. For Ti-Al systems, AM is an efficient technique to combine the properties of both the materials. However, due to large difference in thermal properties of Ti and Al, the chances of cracking increases in the final structure. To overcome this difficulty, few researchers have attempted to fabricate functionally graded Ti-Al structures. Shishkovsky et al. (2012) fabricated functional graded structures in Ti-Al system using direct metal deposition (DMD) technique. The aim was to achieve a controlled development of intermetallic phases in different regions so as to produce a gradation in physical properties in the final structure and avoid formation of cracks. However, the variation in phases was found to be irregular and formation of cracks was observed due to brittle intermetallic phases like TiAl and Ti_3Al (Ref 78). It was suggested that for crack free deposition the substrate should be preheated to 450 $\sim$ 500 °C in DMD processing. One of the recent studies by Hotz et al. (2021) showed that for Ti-Al system the formation of cracks was lesser in step transition (direct deposition of Ti6Al4V on $AlMg_3$ substrate) when compared to graded transition in composition (gradation from AlSi10Mg to Ti6Al4V where AlSi10Mg was deposited first on $AlMg_3$

substrate) (Ref 79). In another study, Ti6Al4V+Al12Si compositionally graded cylindrical structures were fabricated on a Ti6Al4V substrate by Laser powder directed energy deposition (LP-DED) process. High value of hardness was observed at higher laser power due to presence of intermetallic phases and residual stresses (Ref 80). Also, Yan et al. (2017) used a gradient path to join intermetallic materials (Ti4822) with dissimilar materials (Cp-Ti) using LP-DED. The gradation adopted was from 100% Cp-Ti to 100% Ti4822. An increase in hardness for increased wt.% of Ti4822 was observed (Ref 81).

Apart from these, Ti-Nb alloys have proved to be an efficient material for biomedical applications and studies show that these can also be employed in certain aerospace applications (Ref 82). The work reported on these alloys includes fabrication of Ti-26Nb (Fischer et al. 2016 (Ref 83)) and Ti-27.5Nb (Fischer et al. 2017 (Ref 84)) alloy where a fixed composition of Ti and Nb elemental powders was used, whereas an incremental variation in Nb wt% was utilized by Han et al. (2015) (Ref 85) (0, 5, 10, 15, 20 wt.% Nb). These studies correlated the changes in microstructure, mechanical properties and cytocompatibility of these alloys with variation in Nb %. A reduction in elastic modulus was noticed with increase in Nb% from 10 to 20 wt.%, whereas the hardness for Ti-Nb system was found to be higher than Cp-Ti for all wt% of Nb. However, with addition of Nb there were fluctuations in hardness value due to formation of different phases (like $\alpha + \beta$, metastable ω phases). Similar to this, Thoemmes et al. 2016 reported higher microhardness values than Cp-Ti for all compositions varying from 10 to 50 wt.% Nb used in fabrication of Ti-Nb binary as-melt alloys (Ref 86). Moreover, Wang et al. (2017) (Ref 87) utilized 0, 15, 25 and 45 wt.% Nb and reported minimal value of young's modulus for 25 wt.% Nb. They also observed presence of un-melted Nb into the deposit; a study on developing Ti-6Al-4 V to Nb gradient Alloys with Nb % varying from 0 to 100% was conducted by Cheung (2015). In the study it was observed that with increase in Nb wt.% the hardness of the structure decreased when compared to Ti6Al4V alloy due to increase in grain size and porosity increased. The increase in porosity is due to the fact that the amount of power required to melt the powder increases significantly with increase in wt.% Nb in Ti6AlV to Nb gradient alloys. Hence porosity may increase with increase in wt.% Nb if the increase in power is not sufficient. Microstructural examinations were made and changes in crystallographic structures were identified. However no attempt was made to reduce the porosity of the structure (Ref 88). In another study Catherine et al. (2019) compared fabrication of Ti-44Nb alloy of pre-alloyed powder and differential powder injection. A deviation from the expected composition (Ti-44Nb) was encountered as Ti-38Nb alloy was obtained using differential injection. The presence of un-melted Nb was presented as the reason for the deviation (Ref 89).

Another material combination that continues to be a subject of study is Ti-SS FGM system. Studies suggest that stainless steel and Ti alloys cannot be bonded using traditional heat fusion methods (Ref 90). This is mainly due to formation of large number of Ti-based brittle intermetallic phases like, TiCr, TiFe and $TiFe_2$ (Ref 91). These led to generation of residual stresses, excessive interfacial strains and formation of cracks in the material (Ref 92). The solution for this issue is to provide an interlayer metal or for instance a transition composition to prevent the development of intermetallic phases. Sahasrabudhe et al. (2015) (Ref 93) used LP-DED to deposit Ti64 on SS410 substrate with and without an intermediate bond layer. The structure without intermediate layer delaminated after few layers due to formation of brittle intermetallic phases and development of high residual stresses, whereas the structure with NiCr bond layer did not go through delamination and cracking. It was observed that the diffusion of Ti in NiCr region was relatively lower than that of Ni in Ti6Al4V region, which helped in preventing formation of Fe-Ti-based intermetallic phases. Another successful attempt was made by Li et al. (Ref 94) by introducing a transition composition route (Ti-6Al-4V $\rightarrow$ V $\rightarrow$ Cr $\rightarrow$ Fe $\rightarrow$ SS316) to avoid formation of secondary phases between Ti-6Al-4V and SS316 using LP-DED process. In this study, V and Cr were used as transition metals as it is known that V forms stable solid solutions with Ti (Ref 95) and coefficient of thermal expansion (CTE) of V and Ti are comparable. Also, vanadium has been used as interlayer material in development of functionally graded Ti-6Al-4 V to 304L stainless steel system. However, there was formation of intermetallic brittle phases like FeTi and also Fe-V-Cr sigma phase causing cracking in the components. It was suggested by the authors to use alternate composition paths to avoid formation of Fe-V-Cr sigma phase (Ref 96).

Limited literature is available on Ti-Ni-based FGM. However, they are an attractive material combination due to their disparate properties and ability of modern AM techniques to efficiently develop graded materials that can possess blend of these properties like good thermal resistance, which is a characteristic feature of Ni-based alloys (e.g., Invar) and considerable mechanical strength, corrosion resistance and good strength-to-weight ratio provided by Titanium (Ref 106). These features are useful for applications where the components go through large variations in temperature in order to maintain dimensional accuracy and avoid thermal shock (Ref 107). Unfortunately, there are some technical problems with these Ti-Ni-based FGMs which are a matter of study. Works done on combinations such as Ti6Al4V and Inconel 718, and Ti6Al4V and Inconel 625 for fabricating compositionally graded structures by laser metal deposition exhibited formation of macroscopic cracks for specific compositions due to their thermo-physical property mismatch (Ref 59, 71). In a study on Inconel 718–Ti6Al4V bimetallic structures, Onuike and Bandyopadhyay (2018) showed that this issue of cracking can be resolved by the use of a compositional bond layer (CBL) which was a mixture of a third material—vanadium carbide—with the parent alloys to form an intermediate layer used for bonding the two alloys (Ref 108). Other studies on this concept include development of bimetallic structure of TA15 (Ti-6Al-2Zr-1Mo-1V) and Inconel 718 (Inconel 718) through the use of Cu interlayer (Ref 109) and Nb/Cu multi-interlayer (Ref 110). However, in a recent development Meng et al. (2020) (Ref 69) manufactured a FGM from Inconel-625 to Ti6Al4V by laser synchronous preheating and no cracks were found in preheated gradient samples.

The subsequent sections will provide a detailed review of works done in developing Ti-Ni (alloys)-based FGMs using laser-based AM methods exploring the microstructural variations and evolution of different phases, also providing an account of process parameters used and mechanical characteristics of deposited graded materials.

5. Microstructural and Mechanical Characterization of Ti-Ni FGM Systems

The gradation in amount of one of the materials in a system subsequently leads to variation in its microstructural features, which in turn effects the mechanical characteristics of the deposited structure. Hence, it is imperative to understand the variation in microstructure and development of different phases in fabrication of functionally graded (FG) systems. Table 3 summarizes details of material, AM technique, graded composition, processing parameters used and range of hardness encountered in different studies. Figure 2 shows Ti-Ni phase transformation diagram which was initially put forth by Murray (Ref 111) and was later modified by Nagarajan et al. (Ref 112) to include the extension of the other possible phase fields. The development of different phases with varying wt.% of Ni and Ti can be observed. The phase diagram is helpful in understanding the appearance of different phases in Ti-Ni-based FGMs based on the composition in specific regions. However, in ideal case, the development of microstructure and intermetallic phases for gradient composition should be evaluated based on multi-component phase diagrams. But due to lack of thermodynamic data to evaluate phase equilibrium in Ti-Rene88DT, Ti-Inconel 625, Ti-Inconel 718 researchers have referred Ti-Ni binary phase diagram to explain phase evolution in above-mentioned gradient systems. This assumption is supported by the studies on material systems like Ti-Co-Cr, Ti-Ni-Cr (Ref 113) and Ti-Mo-Cr also Ti-Rene88DT and Ti-Inconel625 systems which shows that the main phases present in these are Ti–rich solid solution and Ti-Ni-based compounds. The phase diagram shows a eutectic reaction between β-Ti and Ti_2Ni, a peritectic reaction between Ti_2Ni and TiNi and a eutectoid decomposition of β-Ti. There are four areas of different phases in Ti-Ni system, which include two transient and six stable phases. The phases that are likely to evolve in Ti-Ni graded material system include α-Ti, β-Ti, TiNi, Ti_2Ni, Ti_3Ni_4, $TiNi_3$, γ, where Ti_2Ni, TiNi and $TiNi_3$ are the three main stable intermetallic phases. With the rise of wt.% of Ni, β-Ti phase decreases, whereas the β-Ti+Ti_2Ni eutectic phase increases. At equal Ti-Ni proportions, TiNi phases develop accompanied by Ti_2Ni. With further increase in wt.% of Ni, $TiNi_3$ phase can be observed which then transform to γ phase. With this basic idea of Ti-Ni binary phase diagram in mind, the evolution of different phases in Ti-Ni alloy-based FGMs can be understood.

In a study on FG Ti-Rene88DT superalloy prepared using Laser rapid forming (LRF) from 100 Ti to 60 wt.% Rene88DT, Lin et al. (2006) (Ref 115) observed evolution of a series of different phases along the graded compositions: α $\alpha + \beta$ $\alpha + \beta + Ti_2Ni$ (10 wt.% Rene88DT) $\beta + Ti_2Ni$ (20-40 wt.% Rene88DT) Ti_2Ni + TiNi (50 wt.% Rene88DT) TiNi (60 wt.% Rene88DT). Figure 3 shows optical micrographs at different wt.% of Rene88DT. From Fig. 3 it is suggested that with increase in wt.% of Rene88DT there was a transition in microstructure from cellular to dendritic accompanied by the decrease in cellular spacing. This conclusion was derived based on earlier studies (Ref 116). As mentioned earlier, with further increase in wt% of Rene88DT a series of phases were developed.

This series involved the growth of $\beta + Ti_2Ni$ anomalous eutectic which was discussed by the same team in a different study (Ref 117). The hardness of the FGM was found to greatly depend on the morphology of phases like Ti_2Ni, TiNi and $\alpha + Ti_2Ni$ eutectoid. Also, studies involving comparison of Ti-Ni-based graded materials and homogenous alloys have shown that the dominant phases are same in both systems; however, there was a variation in evolution of different phases (Ref 118).

The Ti-Ni system can also be tailored to obtain properties that are suitable for bio-medical applications (Ref 119). Abioye et al. (2015) successfully developed FG Ni-Ti system using concurrent feeding of Ni powder and commercially pure (CP) Ti wire via direct laser metal deposition process. The microstructural characterization revealed the presence of NiTi and $NiTi_2$ phases where the fraction of $NiTi_2$ decreased and NiTi increased with increase in Ni powder feed rate. Also, these hard phases caused the maximum hardness to rise up to 1.5 times CP Ti (Ref 120). Also alloys like Inconel 718, Inconel 625 have been successfully used to develop graded structures with Ti, but the major issue with these structures is development of cracks at certain compositions due to development of brittle intermetallic phases. Even though the literature available on additively manufactured Ti-Ni(alloy)-based FGM systems are very limited, successful attempts have been made by different authors to eliminate cracking. However this requires additional processing like preheating of the substrate (Ref 59, 109).

Major works in this area are centered on Ti6Al4V-Inconel-based FGMs. Some of the early applications include fabrication of attachment bracket graded from Inconel 718 to Ti6Al4V for joining aeroshell to an integrally stiffened Ti6Al4V tank structure in metallic thermal protection systems. For this purpose, three techniques were employed (LP-DED, flat wire welding, ultrasonic consolidation) by Domack and Baughman (Ref 71). The components fabricated using LP-DED showed coarse dendritic microstructure and considerable elemental segregation corresponding to 10% Ti6Al4V + 90% Inconel 718 composition and for 40-60% Inconel 718, macroscopic cracks appeared in the deposited structure. The authors concluded that the cracks were not a result of metallurgical characteristics. However, it is known that coarse dendritic structures are relatively more susceptible to cracking as compared to equiaxed microstructure (Ref 121, 122). Also, most studies suggest that the formation of cracks is directly related to the evolution of hard and brittle intermetallic phases in the structure and mismatch in their thermo-physical properties.

In response to the issue of cracking in Ti-Ni (alloy)-based FGMs, few successful attempts have been made to reduce or eliminate the cause of crack formation. Pulugurtha (2014) used LP-DED with 3 different gradation chemistries for depositing Ti6Al4V to Inconel 625 graded structure, among them no cracks were developed in only one of the chemistries (0 to 50% Inconel 625 with 10% increments and then directly to 100% Inconel 625) whereas in the other two chemistries, stress induced cracks were observed owing to hot tearing due to thermo-physical property (like CTE) mismatch between the component and clads. The process parameters for above mentioned chemistry required high laser power (1 KW), high travel speed (8.46 mm/s) and high powder feed rate (0.133 g/min as compared to other compositions with 0.033 g/min powder feed rate) and the variation of hardness for the same as a function of distance from the substrate is illustrated in Fig. 4(a). It was observed that the hardness increased with increase in Inconel 625 up to 50% and later remained almost constant in 50-100% Inconel 625 region. Also, it can be observed from Fig. 4(a) that there was little to negligible effect

Table 3 An account of process parameters, composition and mechanical properties of Ti-Ni(alloy)-based FGMs

S No	FGM system	Composition	Powder feed rate, g/min	AM Process	Laser power, KW	Scan speed, mm/s	No. of Layers	Layer Thickness	Hardness	Study	Ref
1	Ti-6Al-4 V/ Invar	100 vol.% Ti-6Al-4 V to 100 vol.% Invar with 3% increment	…	LP-DED	0.9	12.7	75	0.38 mm	382-858 HV	Evolution of different secondary phases and mechanical characteristics	Bobbio et al. (Ref 126)
2	Inconel 718/Ti-6-4	100 vol.% Ti64 to 100 vol.% Inconel 718 with 10% increment	…	LP-DED/Flat wire welding/ Ultrasonic consolidation	…	…	Wall and column shaped graded structures were developed for LP-DED	…	…	The three processes were compared for microstructural characteristics and effectiveness of each process	Domack. 2005 (Ref 71)
3	Ti-Ni	Pure Ti to Ti-50 wt.%Ni	9-10	Laser Rapid Forming (LRF)	2.1-1.9	8-9	…	…	…	The phase transformation and microstructural evolution was analyzed	Xu et al. 2007 (Ref 118)
4	Ti/Rene88DT	100 wt.% Ti to 60 wt% Rene 88DT	8-12	Laser Rapid Forming (LRF)	2.2-1.8	7-10	26	2-6 mm	150-730 HV	Solidification behavior and phase morphological evolution were studied	Lin et al. 2006 (Ref 115)
5	TiC/IN690 MMC	100 vol.% IN-690 to up to 49 vol.% TiC reinforcement	IN690: ≤ 2.1 IN690/TiC: ≤ 8.15	LP-DED	0.35	17	20	0.254 mm	14-42. HRC	TiC reinforced IN690 FGMMCs were developed. Microstructure and mech. Characteristics were studied	Wilson and Shin (Ref 132)
6	Ti6Al4V/ Inconel 625	3 grading chemistries between 100 wt.% Ti64 to 100 wt.% Inconel 625	0.033-0.133	LP-DED	1-0.5	2.2-8.46	60-100	0.6 mm	200-1100VHN (~ 800VHN for crack free deposition)	Crack free graded structures were obtained for specific composition	S.R Pulugurtha (Ref 59)
7	Ni-Ti graded structure	Ni-Ti graded structure where Ni varied from 30 wt.% to 49 wt.%	Powder (Ni) 5-20 g/min Wire (Ti)800 mm/ min	Hybrid powder (Ni) and wire(Cp-Ti) DED	1.4	3.33	40	1 mm	214-620 HV	The microstructure, phase morphology and micro-hardness were characterized	Abioye 2015 (Ref 120)
8	TA15/Inconel 718	100 wt.% TA15 to 100 wt.% Inconel 718 with 20 wt.% increment	5.2-6.4	LP-DED	1.9-1.4	7	24	0.6 mm	380-860 HV	Prepared crack-free FGM via base preheating	Shang 2020 (Ref 123)

Table 3 continued

S No	FGM system	Composition	Powder feed rate, g/min	AM Process	Laser power, KW	Scan speed, mm/s	No. of Layers	Layer Thickness	Hardness	Study
Ref										
9	Ti-6Al-4V/Inconel 718	100% Ti to 100% Inconel 718 with 10% increment till 30% Inconel 718	10	LP-DED	1.8	6	15	0.8 mm	350-1030 HV	Apart from micro-structure, phase morphology and micro-hardness, high-temperature (HT) resistance of FGM was investigated	Ji et al. 2020 (Ref 114)
10	Inconel625 / Ti6Al4V	100% Inconel 625 to 100% Ti64 with 10% increments	16	LP-DED	0.65	8	179	0.3 mm	260-822 HV	Crack free graded structure was prepared using laser synchronous preheating	Meng et al. (2020) (Ref 69)

of change in process parameter like laser power (500-1000 W) on hardness. Moreover, when the substrate was subjected to preheating up to 540 °C, lesser number of cracks with smaller crack opening were revealed. Therefore, it was suggested by the author that longer preheating times are required to achieve equilibrium in the Ti6Al4V substrate before start of LP-DED process (Ref 59).

This outcome was successfully utilized by Shang et al. (2020) to prepare crack free TA15-Inconel 718 FGM via base preheating. Along the same trend line of previously mentioned studies, in this study also cracks developed for un-preheated samples at around 60-80% Inconel 718 and the microstructure consisted of dendritic crystals consisting of Ti_2Ni, TiNi and Cr_2Ti phases due to higher cooling rates leading to higher hardness in this region, whereas for preheated samples the interface consisted of equiaxed crystals and increased amount of eutectic structures which is also helpful in reducing crack sensitivity. Figure 5(a) and (b) shows the difference between microstructure of preheated and un-preheated samples. The base preheating method did not alter the type of phases present and the evolution of phases was in agreement with other studies on same material combination. The phases evolved as: α-Ti α-Ti + Ti_2Ni Ti_2Ni + TiNi Ti_2Ni + TiNi + Ni-γ Ni-γ. This can be confirmed from Fig. 2 representing the phase transformations in Ti-Ni system (Ref 111, 112).

Also, the overall reduction in hardness due to base preheating further prevented development of cracks at critical locations. Figure 4(b) clearly shows this reduction. It is evident from the two hardness vs distance plots that with increase in Inconel wt.% there is an increase in hardness. However, in Fig. 4(b) the hardness reaches a maximum (∼ 800 HV) and then reduces (∼ 500 HV), whereas in Fig. 4(a) the hardness reaches a maximum and remains almost constant there. This difference may be due to variation in material combination and grading systems adopted.

On the same principle Meng et al. (2020) utilized laser synchronous preheating where initially the substrate was heated by laser before start of deposition and then in order to further reduce the cooling rates the gradient layers were also heated at intermediate stages. After complete deposition the top layer was heated for temperature addition. The results of the study showed successful elimination of cracks for the preheated samples (Ref 69). As evident from the studies that the development of cracks is observed for a specific range of composition (around 60 wt.% Ni alloy), hence another way to avoid the formation of cracks is to keep the concentration of Ni-alloy to below 50%. This approach was adopted by Shuwei Ji et al. (2020) (Ref 114) and apart from microstructure and phase morphology, high temperature (HT) resistance of deposited structures were also investigated. The graded specimens were subjected to temperatures 600, 800 and 900 °C for certain duration. It was observed that at temperatures greater than 600 °C the interfacial regions showed different microstructural evolution. Also, at higher temperatures there was development and increase in thickness of diffusion zone at Ti6Al4V and gradient layers. This result is clearly evident from Fig. 6. When the high temperature exposure reaches 800 °C, a diffusion zone develops between the Ti6Al4V and 90% Inconel 718 region. Below 900 °C, the diffusion gets more prominent. Therefore, the diffusion zone gets thicker with the increase in temperature and duration as expected.

Moreover, with increase in Inconel 718% the microhardness was reported to increase which was an expected result and

corresponding to 30% Inconel 718 the possibility of precipitation of phases like TiFe or $TiCr_2$ was suggested based on previous studies (Ref 124, 125). Also, the peak hardness (1030 HV) was observed at 100% Inconel 718 region which primarily consisted of γ-Ni+Laves. The reason suggested for this high value of hardness was dissolution of Ti_2Ni and TiNi phases in γ-Ni matrix causing the rigidity of γ-Ni to further increase. The hardness observed by the authors is much higher than those of other works (Table 3) even though the parameters that have been posed as the reason for this spike in hardness were also documented in those studies where the maximum hardness was in the range of 600-800 HV for crack free deposition.

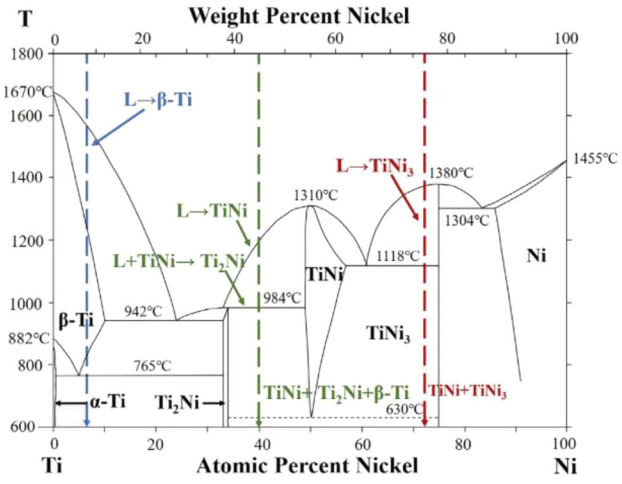

Fig. 2 Phase transformation based on Ti-Ni phase diagram (Ref 114). Reprinted from *Journal of Alloys and Compounds,* Vol 848, S. Ji, Z. Sun, W. Zhang, X. Chen, G. Xie, H. Chang, Microstructural Evolution and High Temperature Resistance of Functionally Graded Material Ti-6Al-4 V/Inconel 718 Coated by Directed Energy Deposition-Laser, Page 156,255, Copyright 2020, with permission from Elsevier

One other important Ni-based alloys include Invar (Fe-36Ni) which possess near zero CTE. Bobbio et al. (2017) (Ref 126) developed Ti6Al4V-Invar 36 graded structure in order to overcome the challenge of joining the two materials having large difference in their thermal properties like CTE. Due to limited thermodynamic database on complete composition range from Ti-6Al-4V to Invar 36 the authors used ternary Fe-Ni-Ti subsystem (Ref 127) to explain the phases developed in the FGM. The microstructure of deposited 100 vol.% Ti region contained columnar prior β-grains with fine α-laths which is a well-documented result (Ref 128 , 129). It was observed that from pure Ti to Fe-36Ni (Invar) the crystal structure changes from HCP to BCC and then to FCC at the end with $>$ 82% Invar.

Also, intermetallic phases (IP) like $NiTi_2$, Ni_3Ti appeared as vol.% of Invar increased and in intermediate compositions, phases like FeTi and Fe_2Ti were observed which was also predicted using calculation of phase diagrams (CALPHAD) in the study. Figure 7 shows electron backscatter diffraction (EBSD) maps of the graded region at different layers. Regions of high hardness were recorded at certain locations owing to the presence of secondary phases and highest average hardness was identified corresponding to 36-48 vol.% Invar. Moreover, major cracking was noted around 64 vol.% Ti6Al4V and 36 vol.% Invar region which was attributed to the mismatch in

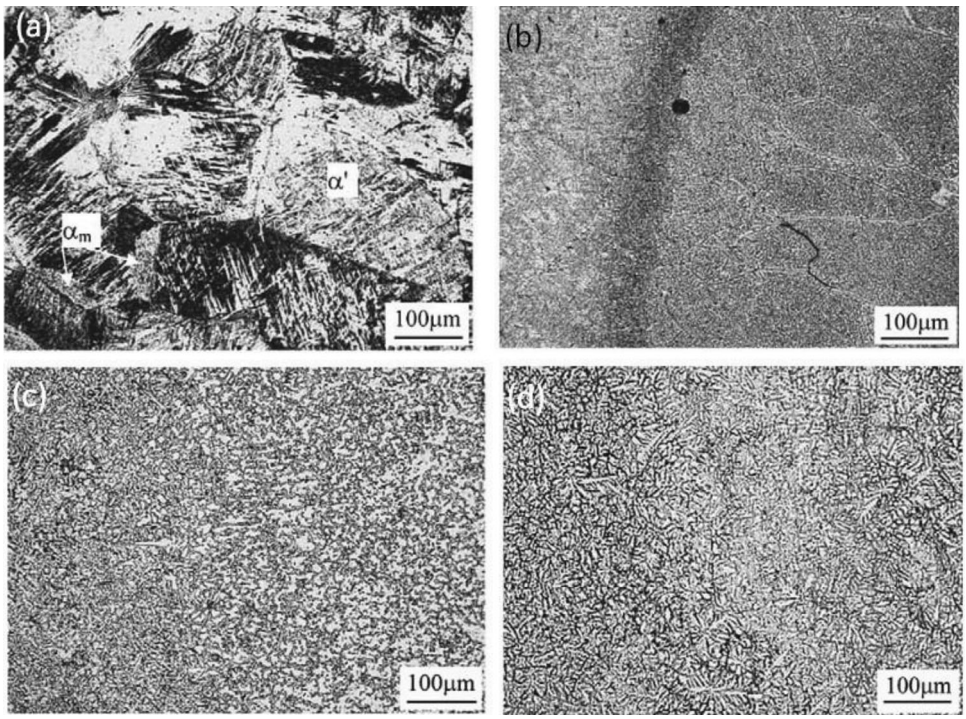

Fig. 3 Optical micrographs at different wt% of Rene88DT. (a) CP Ti, (b) 90%Ti + 10%Rene88DT, (c) 50%Ti + 50%Rene88DT, (d) 40%Ti + 60%Rene88DT (Ref 115). Reprinted from *Acta Materialia,* Vol 54, X. Lin, T.M. Yue, H.O. Yang, W.D. Huang, Microstructure and Phase Evolution in Laser Rapid Forming of a Functionally Graded Ti-Rene88DT Alloy, Pages 1901–1915, Copyright 2006, with permission from Elsevier

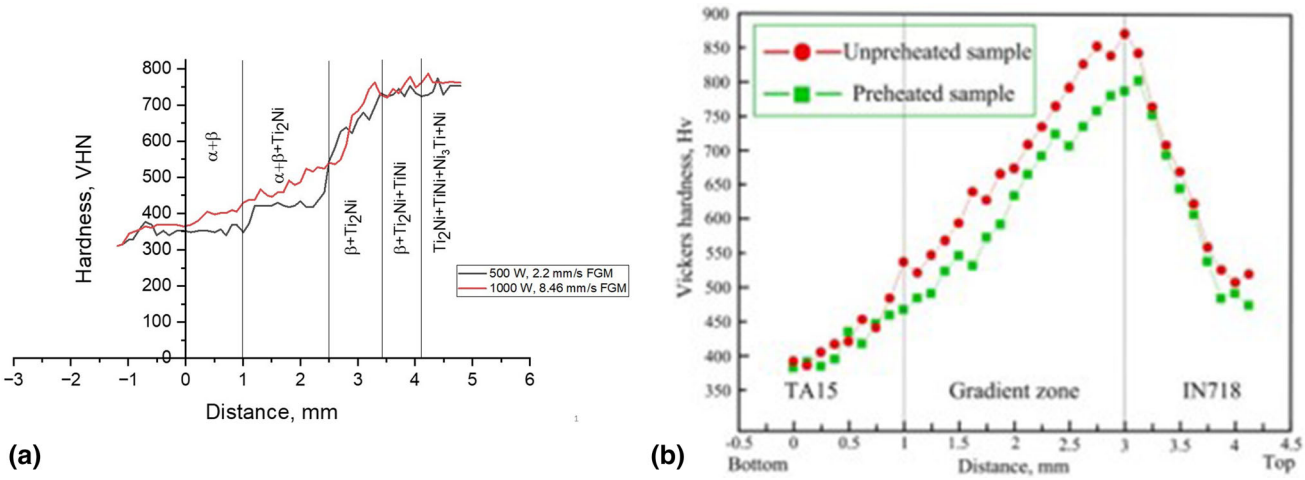

Fig. 4 (a) Hardness values of the Ti-Inconel 625 FGM measured along the composition gradient for 0 to 50% Inconel 625 (Ref 59). (b) Hardness (Vickers) of samples across the gradient zone (TA15-Inconel 718) (Ref 123). Reprinted from *Optics and Laser Technology,* Vol 126, C. Shang, C. Wang, C. Li, G. Yang, G. Xu, J. You, Eliminating the Crack of Laser 3D Printed Functionally Graded Material from TA15 to Inconel718 by Base Preheating, Page 106,100, Copyright 2020, with permission from Elsevier

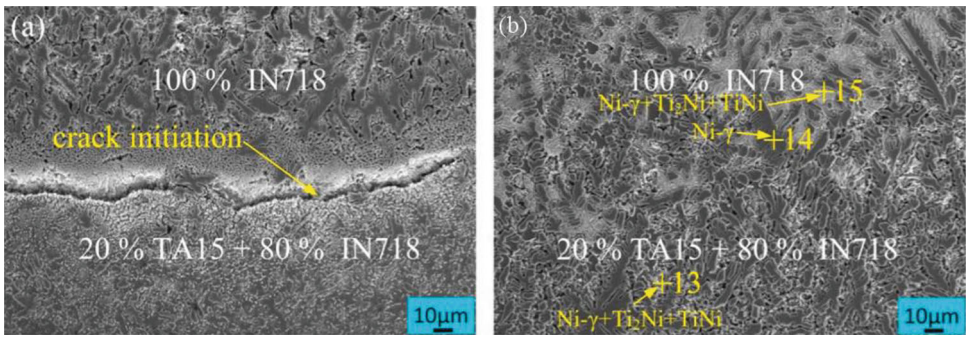

Fig. 5 Microstructure of gradient zone between 20% TA15 + 80% Inconel 718 and 100% Inconel 718 region: (a) without base preheating, (b) with base preheating (Ref 123). Reprinted from *Optics and Laser Technology,* Vol 126, C. Shang, C. Wang, C. Li, G. Yang, G. Xu, J. You, Eliminating the Crack of Laser 3D Printed Functionally Graded Material from TA15 to Inconel718 by Base Preheating, Page 106,100, Copyright 2020, with permission from Elsevier

stiffness and thermal expansion between FeTi and Fe_2Ti phases present, causing stresses to exceed beyond the fracture limit of the material; this conclusion was derived from the works of Ghosh et al. (Ref 130, 131).

6. Summary

In recent years, modern manufacturing of FGMs using AM are being used for several aerospace and aircraft applications. The present review provides an overview of studies on laser-based additive manufacturing techniques used to develop Ti-based FGMs with a primary focus on Ti-Ni FGM systems. It discusses the processing defects, microstructure and mechanical properties of Ti-based FGMs associated with DED. The manufacturing of FGMs by LP-DED is an attractive solution for many engineering applications, thus opening new perspectives for several industrial sectors, such as aerospace, automotive, defense, naval and even in biomedical applications.

The initial section was focused on the concept, basic principle and the conventional methods that have been in use to develop Ti-based FGMs. Later, the advantages and scope of AM techniques were briefly mentioned followed by a detailed discussion on setup, principle and state of the art of LP-DED techniques. Further, the effects of processing parameters (laser power, powder feed rate, scanning speed, etc.) over microstructure, factors like dilution and composition were discussed. In subsequent sections a brief review on different LP-DED techniques used to develop Ti-based FGMs was provided and the significance of Ti-Ni systems in different areas was also discussed followed by a detailed review on microstructural and mechanical characterization of Ti-Ni FGM systems using laser-based AM techniques. FGMs are an innovative material having exceptional strength, stability, corrosion-resistant and light-weight alloy for huge temperature range applications such as aerospace, nuclear power plant and space. Based on this review it can be observed that most of the widest range of FGMs are produced by LP-DED process among the other AM technologies. Thus, the process provides a freedom to design more complex parts, built layer by layer, with strategically controlled compositional variations that enable the directional properties. LP-DED is an efficient method to produce gradient structural properties of any complex parts compared to any other processes.

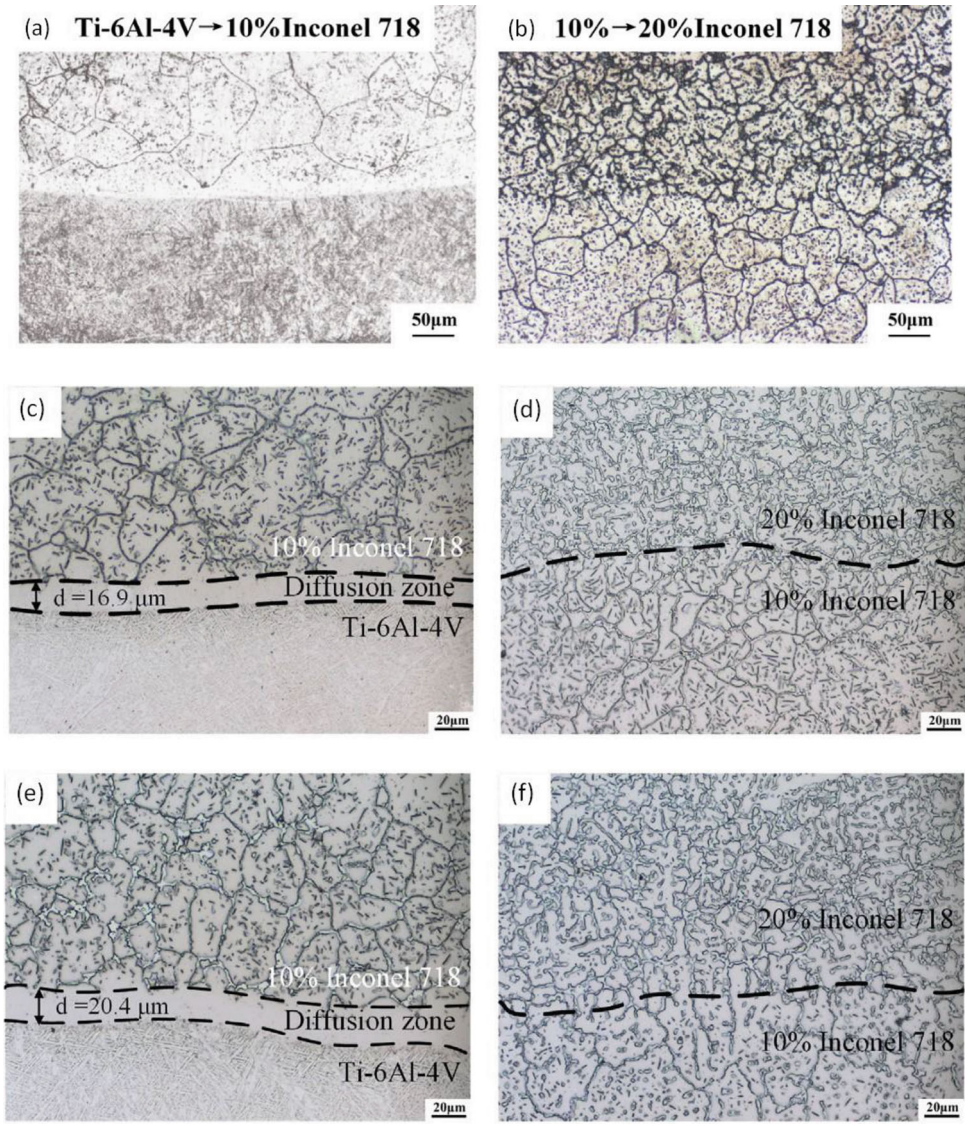

Fig. 6 Microstructure of Ti/10% Inconel 718 and 10/20% Inconel 718 interface (a),(b) without HT exposure, (c),(d) with HT exposure 800 °C/1 h, (e),(f) with HT exposure 800 °C/2 h (Ref 114). Reprinted from *Journal of Alloys and Compounds,* Vol 848, S. Ji, Z. Sun, W. Zhang, X. Chen, G. Xie, H. Chang, Microstructural Evolution and High Temperature Resistance of Functionally Graded Material Ti-6Al-4 V/Inconel 718 Coated by Directed Energy Deposition-Laser, Page 156,255, Copyright 2020, with permission from Elsevier

A complete manufacturing strategy is required to develop defect free, sound metallurgical properties of Ti-based FGMs for intended applications. It indicates that the manufactured Ti FGM components should possess characteristics such as porosity defects free, no lack of fusion, compressive stresses and equiaxed microstructure in all the direction and have uniform microhardness properties linking the favorable mechanical properties.

7. Future Outlook

It is confirmed from the literature reviewed, that there is an increase in the applications of AM technology for the fabrication of FGMs. In a sense, laser directed energy deposition is ideally suited for fabrication of complex geometries with spatially varying distribution of phases that can be engineered to tailor the thermo-mechanical properties in a specific way. Also, it is confirmed that AM technologies can be used to fabricate an almost vast combination of alloys, metals, ceramics and composites in very different geometries. AM technique offers a greater advantage for producing FGM, but there are still number of issues that need to be fixed with this promising technology. Further, research needs to be conducted to generate a comprehensive database and to develop a predictive model for proper process control in AM techniques used to develop FGMs. Additional work should be carried out to improve the process control through development of more powerful feedback control/online monitoring system, in situ analysis for overall FMG fabrication process improvement. This will improve the overall performance of the process, bring down the cost of FGM and improve reliability of the additive manufacturing process. Michgan Tech University have demonstrated low cost metal deposition on moving substrate through DED process (Ref 133). The unified structures with arbitrary

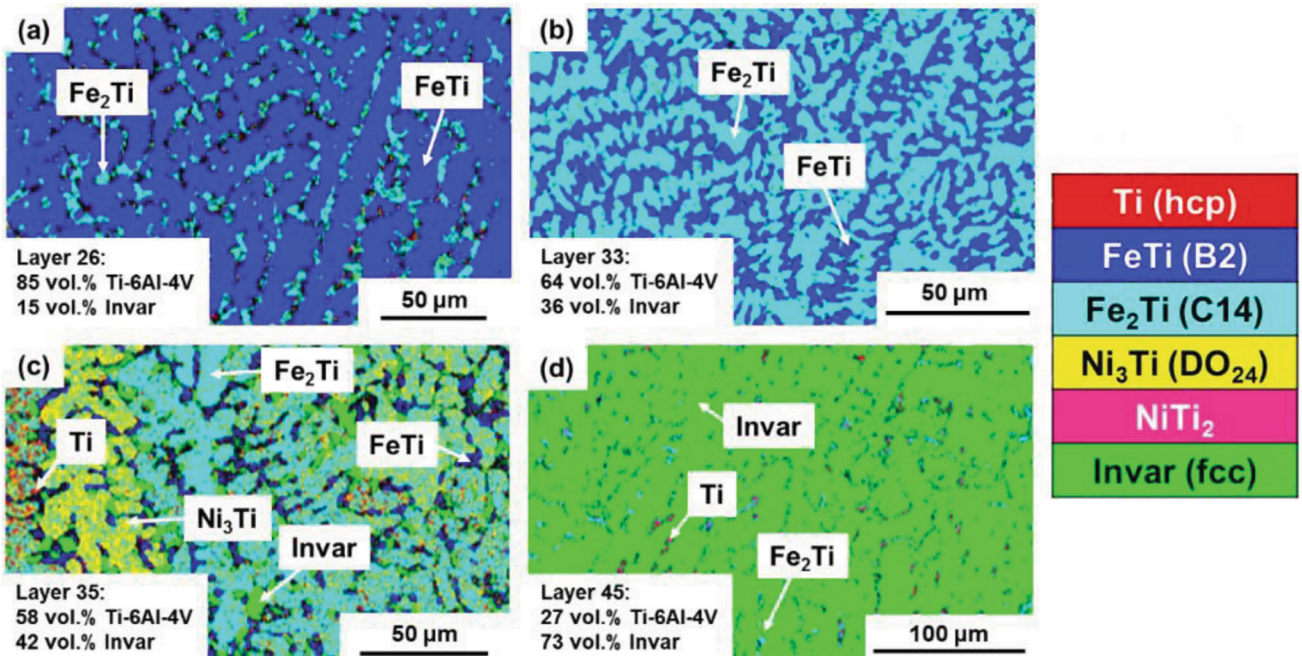

Fig. 7 EBSD phase maps of graded region, (a) shows layer 26 with Fe_2Ti phase present in the interdendritic regions and majority phase as FeTi. (b) Layer 33 consists of FeTi and Fe_2Ti phases. (c) In layer 35, there is a decrease in FeTi and increase in Fe_2Ti phase compared to layer 33, and the FCC Invar phase starts to develop. (d) Layer 45 consisted of fcc Invar as the majority phase with particles of Ni3Ti, FeTi and Fe_2Ti (Ref 126). Reprinted from *Acta Materialia,* Vol 127, L.D. Bobbio, R.A. Otis, J.P. Borgonia, R.P. Dillon, A.A. Shapiro, Z.K. Liu, and A.M. Beese, Additive Manufacturing of a Functionally Graded Material from Ti-6Al-4 V to Invar: Experimental Characterization and Thermodynamic Calculations, Pages 133–142, Copyright 2017, with permission from Elsevier

shapes production of expensive materials through improved buy-to-fly ratio using LP-DED route reduces the manufacturing cost (Ref 33).

Based on the literature available, it is observed that the major issue with fabrication of Ti-Ni (alloy)-based FGMs is development of cracks at specific concentration of Ni (60-80%). However, few studies successfully eliminated the cracks but it required further processing like preheating the substrate. More elaborate research is required to develop adequate processing conditions to eliminate cracking. The inter-pass rolling in LW-DED process can minimize the defects like porosity, residual stresses and distortion of manufactured components. Also, in situ monitoring using visual IR camera, pyrometers, thermocouples and X-rays employment can improve the production quality and the process ability. Apart from this, it was noted that most studies have used minimum incremental gradation of around 10% (vol. or wt.) in the material supplied. The effect of further reducing the gradation ($<$ 10 wt. or vol.%) on the properties can be explored. It is important to generate a universal database for fabrication of different FGM systems, which can include computational modeling FGMs, to optimize the process parameters and to minimize the residual stresses in LP-DED process. The database should contain inspection, testing method and thermo-mechanical, thermodynamic modeling of FGM system. Thermo-mechanical assessment of DED process study pays attention on the deposition parameter analysis such as its strategy, paths, cooling rates and preheating conditions. Also, very few studies have discussed the effects of heat accumulation and intermixing of layers due to remelting up to an extent leading to homogenization of composition in a specific region. Finally, in view of mechanical characterization, most studies have discussed the hardness properties of the deposited material. Therefore, further studies are required to analyze the shear/tensile properties at different environmental conditions. Also, hardness of interface zones, phase formation, grain orientation and fatigue characteristics of Ti-Ni-based FGM systems should be further explored.

However, there are recent advances in science and technology that promise to help circumvent the above challenges. These are described below:

Artificial intelligence (AI) can be adopted in the additive manufacturing industry to help in design aspects and in situ optimization of material and microstructural aspects to precisely develop the desired property gradation in the FGMs. Adoption of machining learning (ML) can take an advantage to predict when the equipment and part fails. ML algorithms can be used for either defect detection or parameter modulation purposes (or both), all with the intent of reducing print failures and saving on time and material costs. The AI can be used where the development of closed-loop control systems has been a key aim for AM engineers. These novel diagnostic technics can be used to properly monitor the process conditions to improve the quality of part fabrication in AM.

Lastly, the design and development of AM techniques that can be used to fabricate multi-functional, intricate and specific application oriented FGMs that can work under extreme working conditions should be explored. In closing, apart from the challenges that persist, application of additive manufacturing to FGMs offers far reaching potential. However, this area needs to be explored further in much more detail.

References

1. G. Henson, Materials for Launch Vehicle Structures, Aerosp. Mater. Appl. p 435–504. (2018) https://doi.org/10.2514/5.9781624104893.0435.0504
2. I. Inagaki, T. Takechi, Y. Shirai and N. Ariyasu, Application and Features of Titanium for the Aerospace Industry, *Nippon Steel Sumitomo Met. Tech. Rep.*, 2014, **106**(106), p 22–27.
3. R.M. Mahamood and E.T. Akinlabi, Functionally Graded Materials, *Springer International Publishing AG*, B. C.P, Ed., 2017, p 1–103
4. M. Koizumi, FGM Activities in Japan, *Compos. Part B Eng*, 1997, **28**(1–2), p 1–4.
5. M.M. Nemat-Alla, M.H. Ata, M.R. Bayoumi and W. Khair-Eldeen, Powder Metallurgical Fabrication and Microstructural Investigations of Aluminum/Steel Functionally Graded Material, *Mater. Sci. Appl.*, 2011, **02**(12), p 1708–1718.
6. M. Sasaki and T. Hirai, Fabrication and Properties Of Functionally Gradient Materials, *J.Ceram. Soc. Japan*, 1991, **99**(1154), p 1002–1013.
7. Y. Watanabe, Y. Inaguma, H. Sato and E. Miura-Fujiwara, A Novel Fabrication Method for Functionally Graded Materials under Centrifugal Force: The Centrifugal Mixed-Powder Method, *Materials*, 2009, **2**(4), p 2510–2525.
8. Y. Watanabe, N. Yamanaka and Y. Fukui, Control of Composition Gradient in a Metal-Ceramic Functionally Graded Material Manufactured by the Centrifugal Method, *Compos. Part A Appl. Sci. Manuf.*, 1998, **29**(5–6), p 595–601.
9. S. El-Hadad, H. Sato, E. Miura-Fujiwara and Y. Watanabe, Fabrication of Al-Al3Ti/Ti3Al Functionally Graded Materials under a Centrifugal Force, *Materials*, 2010, **3**(9), p 4639–4656.
10. M. Sathish, N. Radhika and B. Saleh, A Critical Review on Functionally Graded Coatings: Methods, Properties, and Challenges, *Compos. Part B Eng.*, 2021, **2021**(225), p 109278. https://doi.org/10.1016/j.compositesb.2021.109278
11. J.F. Groves and H.N.G. Wadley, Functionally Graded Materials Synthesis via Low Vacuum Directed Vapor Deposition, *Compos. Part B Eng.*, 1997, **28**(1–2), p 57–69.
12. R.M. Mahamood, E.T. Akinlabi, M. Shukla and S. Pityana, Functionally Graded Material: An Overview, *Lect. Notes Eng. Comput. Sci.*, 2012, **3**, p 1593–1597.
13. G.E. Knoppers, J.W. Gunnink, J. Van Den Hout, and W.P. Van Vliet, The Reality of Functionally Graded Material Products, in Proc. Solid Free. Fabr. Symp., (2004), p 38–43
14. M. Kawase, T. Tago, M. Kurosawa, H. Utsumi and K. Hashimoto, Chemical Vapor infiltration and Deposition to Produce a Silicon Carbide-Carbon Functionally Gradient Material, *Chem. Eng. Sci.*, 1999, **54**(15–16), p 3327–3334.
15. M. Jain, R.K. Sadangi, W.R. Cannon and B.H. Kear, Processing of Functionally Graded Wc/Co/Diamond Nanocomposites, *Scr. Mater.*, 2001, **44**(8–9), p 2099–2103.
16. C.Q. Hong, X.H. Zhang, W.J. Li, J.C. Han and S.H. Meng, A Novel Functionally Graded Material in the Zrb2-sic and Zro2 System by Spark Plasma Sintering, *Mater. Sci. Eng. A*, 2008, **498**(1–2), p 437–441.
17. L. Yongming, P. Wei, L. Shuqin, W. Ruigang and L. Jianqiang, A Novel Functionally Graded Materials in the Ti–Si–C System, *Mater. Sci. Eng. A*, 2003, **345**(1–2), p 99–105.
18. X. Tang, H. Zhang, D. Du, D. Qu, C. Hu, R. Xie and Y. Feng, Fabrication of W-Cu Functionally Graded Material by Spark Plasma Sintering Method, *Int. J. Refract. Met. Hard Mater.*, 2014, **42**, p 193–199. https://doi.org/10.1016/j.ijrmhm.2013.09.005
19. S.H. Lee, H. Tanaka and Y. Kagawa, Spark Plasma Sintering and Pressureless Sintering of SiC using Aluminum Borocarbide Additives, *J. Eur. Ceram. Soc.*, 2009, **29**(10), p 2087–2095.
20. T.P.D. Rajan, R.M. Pillai and B.C. Pai, Characterization of Centrifugal Cast Functionally Graded Aluminum-Silicon Carbide Metal Matrix Composites, *Mater. Charact.*, 2010, **61**(10), p 923–928. https://doi.org/10.1016/j.matchar.2010.06.002
21. J. Ma and G.E.B. Tan, Processing and Characterization of Metal-Ceramics Functionally Gradient Materials, *J. Mater. Process. Technol.*, 2001, **113**(1–3), p 446–449.
22. W.A. Gooch, B.H.C. Chen, M.S. Burkins, R. Palicka, J. Rubin and R. Ravichandran, Development and Ballistic Testing of a Functionally Gradient Ceramic/Metal Applique, *Mater. Sci. Forum*, 1999, **308–311**, p 614–621.
23. A.K. Sachdev, K. Kulkarni, Z.Z. Fang, R. Yang and V. Girshov, Titanium for Automotive Applications: Challenges and Opportunities in Materials and Processing, *Jom*, 2012, **64**(5), p 553–565.
24. Y.M. Lim, Y.J. Park, Y.H. Yun and K.S. Hwang, Functionally Graded Ti/HAP Coatings on Ti-6Al-4V Obtained by Chemical Solution Deposition, *Ceram. Int.*, 2002, **28**(1), p 37–41.
25. M. Jayachandran, H. Tsukamoto, H. Sato and Y. Watanabe, Formation Behavior of Continuous Graded Composition in Ti-ZrO 2 Functionally Graded Materials Fabricated by Mixed-Powder Pouring Method, *J. Nanomater.*, 2013, **2013**, p 1–8. https://doi.org/10.1155/2013/504631
26. G. Batin and C. Popa, Mechanical Properties of Ti/HA Functionally Graded Materials for Hard Tissue Replacement, *Powder Metall. Prog.*, 2011, **11**(3), p 206–209.
27. T. Fujii, K. Tohgo, M. Iwao and Y. Shimamura, Fracture Toughness Distribution of Alumina-Titanium Functionally Graded Materials Fabricated by Spark Plasma Sintering, *J. Alloys Compd.*, 2018, **766**, p 1–11. https://doi.org/10.1016/j.jallcom.2018.06.304
28. K.B. Panda and K.S. Ravi Chandran, Titanium-Titanium Boride (Ti-TiB) Functionally Graded Materials Through Reaction Sintering: Synthesis, Microstructure, and Properties, *Metall. Mater. Trans.A*, 2003, **34**(9), p 1993–2003. https://doi.org/10.1007/s11661-003-0164-3
29. X.H. Zhang, J.C. Han, S.Y. Du and J.V. Wood, Microstructure and Mechanical Properties of TiC-Ni Functionally Graded Materials by Simultaneous Combustion Synthesis and Compaction, *J. Mater. Sci.*, 2000, **35**(8), p 1925–1930.
30. A. Reichardt, A.A. Shapiro, R. Otis, R.P. Dillon, J.P. Borgonia, B.W. McEnerney, P. Hosemann and A.M. Beese, Advances in Additive Manufacturing of Metal-Based Functionally Graded Materials, *Int. Mater. Rev.*, 2021, **66**(1), p 1–29.
31. C. Zhang, F. Chen, Z. Huang, M. Jia, G. Chen, Y. Ye, Y. Lin, W. Liu, B. Chen, Q. Shen, L. Zhang and E.J. Lavernia, Additive Manufacturing of Functionally Graded Materials: A Review, *Mater. Sci. Eng. A*, 2019, **764**, p 138209. https://doi.org/10.1016/j.msea.2019.138209
32. L. Yang, K. Hsu, B. Baughman, D. Godfrey, F. Medina, M. Menon, and S. Wiener, Electron Beam Technology, (2017), p 1–29, https://doi.org/10.1007/978-3-319-55128-9_4
33. D.-G. Ahn, Directed Energy Deposition (DED) Process: State of the Art, *Int. J. Precis. Eng. Manuf. Technol.*, 2021, **8**, p 703–742.
34. I. Harter, Method of Forming Structures Wholly Of Fusion Deposited Weld Metal, U.S. Patent 2,299,747, 1942
35. A. Kratky, Production of Hard Metal Alloys, U.S. Patent 2,076,952, 1937
36. B.H.K. C.O. Brown, E.M. Breinan, Method for Fabricating Articles by Sequential Layer Deposition, U.S. Patent 4,323,756A, 1982
37. E.B.C. P.P. Mehta, R.R. Otten, Method and Apparatus for Repairing Metal in an Article, U.S. Patent 4,743,733A, 1988
38. H.-J.H. W. Konig, T. Celiker, Approaches to Prototyping of Metallic Parts, in 2nd Eur. Conf. Rapid Prototyp. Manuf., (Nottingham, UK, 1993), pp. 303–316
39. W.M. F. Klocke, H. Wirtz, Direct Manufacturing of Metal Prototypes and Prototype Tools, in 7th Solid Free. Fabr. Symp., (Austin, USA, 1996), pp. 141–148
40. A.W. Hammeke, Laser Spray Nozzle and Method, U.S. Patent 4,724,299A, 1988
41. A. Buongiorno, Laser/Powdered Metal Cladding Nozzle, U.S. Patent 5,477,026A, 1995
42. D. Jafari, T.H.J. Vaneker and I. Gibson, Wire and Arc Additive Manufacturing: Opportunities and Challenges to Control the Quality and Accuracy of Manufactured Parts, *Mater. Des.*, 2021, **202**, 109471. https://doi.org/10.1016/j.matdes.2021.109471
43. I. Gibson, D. Rosen, and B. Stucker, "Directed Energy Deposition Processes.Additive Manufacturing Technologies" Springer, Newyork, p 245-268 https://doi.org/10.1007/978-1-4939-2113-3
44. L. Xue and M.U. Islam, Laser Consolidation–A Novel One-Step Manufacturing Process for Making Net-Shape Functional Components, Spec. Meet. Cost Eff. Manuf. via Net Shape Process, (2006), p 15:1–14
45. F. Mazzucato, S. Tusacciu, M. Lai, S. Biamino, M. Lombardi and A. Valente, Monitoring Approach to Evaluate the Performances of a New

Deposition Nozzle Solution for DED Systems, *Technologies*, 2017, **5**(2), p 29. https://doi.org/10.3390/technologies5020029
46. T. Schopphoven, A. Gasser and G. Backes, EHLA: Extreme High-Speed Laser Material Deposition: Economical and Effective Protection Against Corrosion and Wear, *Laser Tech. J.*, 2017, **14**(4), p 26–29.
47. F. Wang, J. Mei and X. Wu, Compositionally Graded Ti6Al4V+TiC Made by Direct Laser Fabrication Using Powder and Wire, *Mater. Des.*, 2007, **28**(7), p 2040–2046.
48. A. Heralić, A.K. Christiansson and B. Lennartson, Height Control of Laser Metal-Wire Deposition Based on Iterative Learning Control and 3D Scanning, *Opt. Lasers Eng.*, 2012, **50**(9), p 1230–1241.
49. L.P. Raut and R.V. Taiwade, Wire Arc Additive Manufacturing: a Comprehensive Review and Research Directions, *J. Mater. Eng. Perform.*, 2021, **30**(7), p 4768–4791. https://doi.org/10.1007/s11665-021-05871-5
50. D. Ding, Z. Pan, D. Cuiuri and H. Li, Wire-Feed Additive Manufacturing of Metal Components: Technologies, Developments and Future Interests, *Int. J. Adv. Manuf. Technol.*, 2015, **81**(1–4), p 465–481.
51. M.L. Griffith, M.E. Schlieriger, L.D. Harwell, M.S. Oliver, M.D. Baldwin, M.T. Ensz, M. Essien, J. Brooks, C.V. Robino, J.E. Smugeresky, W.H. Hofmeister, M.J. Wert and D.V. Nelson, Understanding Thermal Behavior in the LENS Process, *Mater. Des.*, 1999, **20**(2–3), p 107–113.
52. L. Bian, S.M. Thompson and N. Shamsaei, Mechanical Properties and Microstructural Features of Direct Laser-Deposited Ti-6Al-4V, *Jom*, 2015, **67**(3), p 629–638.
53. A. Harooni, A.M. Nasiri, A.P. Gerlich, A. Khajepour, A. Khalifa and J.M. King, Processing Window Development for Laser Cladding of Zirconium on Zirconium Alloy, *J. Mater. Process. Technol.*, 2016, **230**, p 263–271.
54. S. Ocylok, E. Alexeev, S. Mann, A. Weisheit, K. Wissenbach and I. Kelbassa, Correlations of Melt Pool Geometry and Process Parameters During Laser Metal Deposition by Coaxial Process Monitoring, *Phys. Proc.*, 2014, **56**, p 228–238. https://doi.org/10.1016/j.phpro.2014.08.167
55. I. Garmendia, J. Leunda, J. Pujana and A. Lamikiz, In-Process Height Control During Laser Metal Deposition Based on Structured Light 3D Scanning, *Proc. CIRP*, 2018, **68**, p 375–380. https://doi.org/10.1016/j.procir.2017.12.098
56. S. Huang, D. Li, L. Zhang, X. Zhang and W. Zhu, Tailoring the Mechanical Properties of Laser Cladding-Deposited Ferrous Alloys with a Mixture of 410l Alloy and Fe-Cr-B-Si-Mo Alloy Powders, *Materials*, 2019, **12**(3), p 410. https://doi.org/10.3390/ma12030410
57. T. Grandal, A. Zornoza, S. Fraga, G. Castro, T. Sun and K.T.V. Grattan, Laser Cladding-Based Metallic Embedding Technique for Fiber Optic Sensors, *J. Light. Technol.*, 2018, **36**(4), p 1018–1025.
58. H. Alemohammad, E. Toyserkani and C.P. Paul, Fabrication of Smart Cutting Tools with Embedded Optical Fiber Sensors using Combined Laser Solid Freeform Fabrication and Moulding Techniques, *Opt. Lasers Eng.*, 2007, **45**(10), p 1010–1017.
59. S.R. Pulugurtha, Functionally Graded Ti6al4v And Inconel 625 By Laser Metal Deposition, (2014), p 207, http://scholarsmine.mst.edu/cgi/viewcontent.cgi?article=3334&context=doctoral_dissertations
60. Z. Feng, *Processes and Mechanisms of Welding Residual Stress and Distortion*, Elsevier Science Publisher, Netherlands, 2005, p p364
61. L. Sexton, S. Lavin, G. Byrne and A. Kennedy, Laser Cladding of Aerospace Materials, *J. Mater. Process. Technol.*, 2002, **122**(1), p 63–68.
62. R.R. Unocic and J.N. DuPont, Process Efficiency Measurements in the Laser Engineered Net Shaping Process, *Metall. Mater. Trans. B*, 2004, **35**(1), p 143–152. https://doi.org/10.1007/s11663-004-0104-7
63. R.M. Mahamood, *Laser Metal Deposition Process of Metals, Alloys, and Composite Materials, Engineering Materials and Processes*, Springer International Publishing AG, Cham, 2018, p 62
64. S.R. Pulugurtha, J. Newkirk, F. Liou and H.N. Chou, Functionally Graded Materials by Laser Metal Deposition 20th Annu, *Int. Solid Free. Fabr. Symp. SFF*, 2009, **2009**, p 454–469.
65. M. Picasso, C.F. Marsden, J.D. Wagniere, A. Frenk and M. Rappaz, A Simple but Realistic Model for Laser Cladding, *Metall. Mater. Trans. B*, 1994, **25**(2), p 281–291.
66. V. Fallah, M. Alimardani, S.F. Corbin and A. Khajepour, Impact of Localized Surface Preheating on the Microstructure and Crack Formation in Laser Direct Deposition of Stellite 1 on AISI 4340 Steel, *Appl. Surf. Sci.*, 2010, **257**(5), p 1716–1723. https://doi.org/10.1016/j.apsusc.2010.09.003
67. R. Jendrzejewski, G. Sliwinski, A. Conde and J.J. de Damborenea, Influence of the Base Preheating on Cracking of the Laser-Cladded Coatings, *Laser Process. Adv. Mater. Laser Microtechnol.*, 2003, **5121**, p 356.
68. Y.J. Chen, T.M. Yue and Z.N. Guo, Laser Joining of Metals to Plastics with Ultrasonic Vibration, *J. Mater. Process. Technol.*, 2017, **249**, p 441–451. https://doi.org/10.1016/j.jmatprotec.2017.06.036
69. W. Meng, Y. Xiaohui, W. Zhang, F. Junfei, G. Lijie, M. Qunshuang and C. Bing, Additive Manufacturing of a Functionally Graded Material from Inconel625 to Ti6Al4V by Laser Synchronous Preheating, *J. Mater. Process. Technol.*, 2020, **275**, p 116368.
70. S. Ravichandran, Thermal Residual Stresses in a Functionally Graded Material, *System*, 1995, **201**, p 269–276.
71. M.S. Domack and J.M. Baughman, Development of Nickel-Titanium Graded Composition Components, *Rapid Prototyp. J.*, 2005, **11**(1), p 41–51.
72. A. Singh, S. Kapil and M. Das, A Comprehensive Review of the Methods and Mechanisms for Powder Feedstock Handling in Directed Energy Deposition, *Addit. Manuf.*, 2020, **35**, p 101388. https://doi.org/10.1016/j.addma.2020.101388
73. N. Noda, Thermal Stresses in Functionally Graded Materials, *J. Therm. Stress.*, 1999, **22**(4–5), p 477–512.
74. E. Brandl, B. Baufeld, C. Leyens and R. Gault, Additive Manufactured Ti-6Al-4V using Welding Wire: Comparison of Laser and Arc Beam Deposition and Evaluation with Respect to Aerospace Material Specifications, *Phys. Proc.*, 2010, **5**, p 595–606. https://doi.org/10.1016/j.phpro.2010.08.087
75. A.G. Ermachenko, R.Y. Lutfullin and R.R. Mulyukov, Advanced Technologies of Processing Titanium Alloys and their Applications in Industry, *Rev. Adv. Mater. Sci.*, 2011, **29**(1), p 68–82.
76. J.C. Williams and R.R. Boyer, Opportunities and Issues in the Application of Titanium Alloys for Aerospace Components, *Metals*, 2020, **10**(6), p 705. https://doi.org/10.3390/met10060705
77. V.A. Afanas'ev, P.V. Nikitin and O.V. Tushavina, Behavior of Titanium Alloys in Aerodynamic Heating of Hypersonic Airplanes, *Russ. Eng. Res.*, 2019, **39**(1), p 25–30. https://doi.org/10.3103/S1068798X1901012X
78. I. Shishkovsky, F. Missemer and I. Smurov, Direct Metal Deposition of Functional Graded Structures in Ti- Al System, *Phys. Proc.*, 2012, **39**, p 382–391.
79. H. Hotz, M. Zimmermann, S. Greco, B. Kirsch and J.C. Aurich, Additive Manufacturing of Functionally Graded Ti-Al Structures by Laser-Based Direct Energy Deposition, *J. Manuf. Process.*, 2021, **68**, p 1524–1534. https://doi.org/10.1016/j.jmapro.2021.06.068
80. Y. Zhang and A. Bandyopadhyay, Direct Fabrication of Bimetallic Ti6Al4V+Al12Si Structures via Additive Manufacturing, *Addit. Manuf.*, 2019, **29**, p 100783. https://doi.org/10.1016/j.addma.2019.100783
81. L. Yan, X. Chen, Y. Zhang, J.W. Newkirk and F. Liou, Fabrication of Functionally Graded Ti and γ-TiAl by Laser Metal Deposition, *Jom*, 2017, **69**(12), p 2756–2761.
82. G.V. Martins, C.R.M. Silva, C.A. Nunes, V.J. Trava-Airoldi, L.A. Borges and J.P.B. Machado, Beta Ti-45Nb and Ti-50Nb Alloys Produced by Powder Metallurgy for Aerospace Application, *Mater. Sci. Forum*, 2010, **660–661**, p 405–409.
83. M. Fischer, D. Joguet, G. Robin, L. Peltier and P. Laheurte, In Situ Elaboration of a Binary Ti–26Nb Alloy by Selective Laser Melting of Elemental Titanium and Niobium Mixed Powders, *Mater. Sci. Eng. C*, 2016, **62**, p 852–859. https://doi.org/10.1016/j.msec.2016.02.033
84. M. Fischer, P. Laheurte, P. Acquier, D. Joguet, L. Peltier, T. Petithory, K. Anselme and P. Mille, Synthesis and Characterization of Ti-27.5Nb Alloy Made by CLAD® Additive Manufacturing Process for Biomedical Applications, *Mater. Sci. Eng. C*, 2017, **75**, p 341–348. https://doi.org/10.1016/j.msec.2017.02.060
85. M.K. Han, J.Y. Kim, M.J. Hwang, H.J. Song and Y.J. Park, Effect of Nb on the Microstructure, Mechanical Properties, Corrosion Behavior, and Cytotoxicity of Ti-Nb Alloys, *Materials*, 2015, **8**(9), p 5986–6003.
86 .A. Thoemmes, I.A. Bataev, N.S. Belousova, and D. V. Lazurenko, Microstructure and Mechanical Properties of Binary Ti-Nb Alloys for

Application in Medicine, in Proc.-2016 11th Int. Forum Strateg. Technol. IFOST, 2017, p 26–29
87. Q. Wang, C. Han, T. Choma, Q. Wei, C. Yan, B. Song and Y. Shi, Effect of Nb Content on Microstructure, Property and in Vitro Apatite-Forming Capability of Ti-Nb Alloys Fabricated via Selective Laser Melting, *Mater. Des.*, 2017, **126**, p 268–277. https://doi.org/10.1016/j.matdes.2017.04.026
88. C. Cheung, *Characterization of Laser Deposited Ti-6Al-4V to Nb Gradient Alloys*, CAL POLY STATE Univ, California, 2015, p 3–5
89. C. Schneider-Maunoury, L. Weiss, O. Perroud, D. Joguet, D. Boisselier and P. Laheurte, An Application of Differential Injection to Fabricate Functionally Graded Ti-Nb Alloys using DED-CLAD ®process, *J. Mater. Process. Technol.*, 2019, **268**, p 171–180. https://doi.org/10.1016/j.jmatprotec.2019.01.018
90. Z. Sun and R. Karppi, The Application of Electron Beam Welding for the Joining of Dissimilar Metals: An Overview, *J. Mater. Process. Technol.*, 1996, **59**(3), p 257–267. https://doi.org/10.1016/0924-0136(95)02150-7
91. P. Li, J. Li, J. Xiong, F. Zhang and S.H. Raza, Diffusion Bonding Titanium to Stainless Steel using Nb/Cu/Ni Multi-Interlayer, *Mater. Charact.*, 2012, **68**, p 82–87. https://doi.org/10.1016/j.matchar.2012.03.016
92. G. Göbel, J. Kaspar, T. Herrmannsdörfer, B. Brenner, and E. Beyer, Insights into Intermetallic Phases on Pulse Welded Dissimilar Metal Joints. in 4th Int. Conf. High Speed Form, 2010, (May 2016), p 127–136
93. H. Sahasrabudhe, R. Harrison, C. Carpenter and A. Bandyopadhyay, Stainless Steel to Titanium Bimetallic Structure using LENS™, *Addit. Manuf.*, 2015, **5**, p 1–8. https://doi.org/10.1016/j.addma.2014.10.002
94. W. Li, S. Karnati, C. Kriewall, J. Frank Liou, K.M. Newkirk, B. Taminger and W.J. Seufzer, Fabrication and Characterization of a Functionally Graded Material from Ti-6Al-4V to SS316 by Laser Metal Deposition, *Addit. Manuf.*, 2017, **14**, p 95–104. https://doi.org/10.1016/j.addma.2016.12.006
95. P.C. Collins, R. Banerjee, S. Banerjee and H.L. Fraser, Laser Deposition of Compositionally Graded Titanium-Vanadium and Titanium-Molybdenum Alloys, *Mater. Sci. Eng. A*, 2003, **352**(1–2), p 118–128.
96. A. Reichardt, R.P. Dillon, J.P. Borgonia, A.A. Shapiro, B.W. McEnerney, T. Momose and P. Hosemann, Development and Characterization of Ti-6Al-4V to 304L Stainless Steel Gradient Components Fabricated with Laser Deposition Additive Manufacturing, *Mater. Des.*, 2016, **104**, p 404–413. https://doi.org/10.1016/j.matdes.2016.05.016
97. D.C. Hofmann, S. Roberts, R. Otis, J. Kolodziejska, R.P. Dillon, J.O. Suh, A.A. Shapiro, Z.K. Liu and J.P. Borgonia, Developing Gradient Metal Alloys Through Radial Deposition Additive Manufacturing, *Sci. Rep.*, 2014, **4**(1), p 1–8.
98. R. Banerjee, P.C. Collins, D. Bhattacharyya, S. Banerjee and H.L. Fraser, Microstructural Evolution in Laser Deposited Compositionally Graded α/β Titanium-Vanadium Alloys, *Acta Mater.*, 2003, **51**(11), p 3277–3292.
99. C.G. Wenjun Ge, Feng Lin, Functional Gradient Material Of Ti-6al-4v And γ- Fabricated by Electron Beam Selective Melting Functional Gradient Material of Ti-6Al-4V and γ-TiAl Fabricated by Electron Beam Selective Melting. in International Solid Freeform Fabrication Symposium. (University of Texas, Austin, 2015), 602–613
100. Y. Liu, C. Liu, W. Liu, Y. Ma, C. Zhang, Q. Cai and B. Liu, Microstructure and Properties of Ti/Al Lightweight Graded Material by Direct Laser Deposition, *Mater. Sci. Technol.*, 2018, **34**(8), p 945–951. https://doi.org/10.1080/02670836.2017.1412042
101. C. Schneider-Maunoury, L. Weiss, P. Acquier, D. Boisselier and P. Laheurte, Functionally Graded Ti6Al4V-Mo Alloy Manufactured with DED-CLAD® Process, *Addit. Manuf.*, 2017, **17**, p 55–66. https://doi.org/10.1016/j.addma.2017.07.008
102. Y. Geng, W. Xie, Y. Tu, S. Deng, D. Egan, D.P. Dowling, H. Song, S. Zhang and N. Harrison, Ti–6Al–4V Microstructural Functionally Graded Material by Additive Manufacturing: Experiment and Computational Modelling, *Mater. Sci. Eng. A*, 2021, **823**, p 141782. https://doi.org/10.1016/j.msea.2021.141782
103. L. Li, J. Wang, P. Lin and H. Liu, Microstructure and Mechanical Properties of Functionally Graded TiCp/Ti6Al4V Composite Fabricated by Laser Melting Deposition, *Ceram. Int.*, 2017, **43**(18), p 16638–16651. https://doi.org/10.1016/j.ceramint.2017.09.054
104. L.D. Bobbio, B. Bocklund, R. Otis, J.P. Borgonia, R. Peter Dillon, A.A. Shapiro, B. McEnerney, Z.K. Liu and A.M. Beese, Characterization of a Functionally Graded Material of Ti-6Al-4V to 304L Stainless Steel with an Intermediate V Section, *J. Alloys Compd.*, 2018, **742**, p 1031–1036. https://doi.org/10.1016/j.jallcom.2018.01.156
105. K. Zhao, G. Zhang, G. Ma, C. Shen and D. Wu, Microstructure and Mechanical Properties of Titanium Alloy/Zirconia Functionally Graded Materials Prepared by Laser Additive Manufacturing, *J. Manuf. Process.*, 2020, **56**(May), p 616–622. https://doi.org/10.1016/j.jmapro.2020.05.044
106. M. Peters, J. Hemptenmacher, J. Kumpfert and C. Leyens, *Structure and Properties of Titanium and Titanium Alloys, Titanium and Titanium Alloys*, Wiley-VCH Verlag GmbH & Co. KGaA, Weinheim FRG p, 2005, p 1–36
107. R. Roy, D.K. Agrawal and H.A. McKinstry, Very Low Thermal Expansion Coefficient Materials, *Annu. Rev. Mater. Sci.*, 1989, **19**(1), p 59–81. https://doi.org/10.1146/annurev.ms.19.080189.000423
108. B. Onuike and A. Bandyopadhyay, Additive Manufacturing of Inconel 718–Ti6Al4V Bimetallic Structures, *Addit. Manuf.*, 2018, **22**, p 844–851. https://doi.org/10.1016/j.addma.2018.06.025
109. C. Shang, G. Xu, C. Wang, G. Yang and J. You, Laser Deposition Manufacturing of Bimetallic Structure from TA15 to Inconel 718 via Copper Interlayer, *Mater. Lett.*, 2019, **252**, p 342–344. https://doi.org/10.1016/j.matlet.2019.06.030
110. C. Shang, C. Wang, G. Xu, C. Li and J. You, Laser Additive Manufacturing of TA15 - Inconel 718 Bimetallic Structure via Nb/Cu Multi-Interlayer, *Vacuum*, 2019, **169**, p 108888. https://doi.org/10.1016/j.vacuum.2019.108888
111. L.Joanne Murray, Phase Diagrams of Binary Titanium Alloys, Metals Park, OH, (1987)
112. R. Nagarajan and S. Ranganathan, A Study of the Glass-Forming Range in the Ternary TiNiAl System by Mechanical Alloying, *Mater. Sci. Eng. A*, 1994, **179–180**, p 168–172. https://doi.org/10.1016/0921-5093(94)90186-4
113. K.P. Gupta, The Cr-Ni-Ti (Chromium-Nickel-Titanium) System–Update, *J. Phase Equilibria.*, 2003, **24**(1), p 86–89.
114. S. Ji, Z. Sun, W. Zhang, X. Chen, G. Xie and H. Chang, Microstructural Evolution and High Temperature Resistance of Functionally Graded Material Ti-6Al-4V/Inconel 718 Coated by Directed Energy Deposition-Laser, *J. Alloys Compd.*, 2020, **2020**(848), p 156255. https://doi.org/10.1016/j.jallcom.2020.156255
115. X. Lin, T.M. Yue, H.O. Yang and W.D. Huang, Microstructure and Phase Evolution in Laser Rapid Forming of a Functionally Graded Ti-Rene88DT Alloy, *Acta Mater.*, 2006, **54**(7), p 1901–1915.
116. D. Fisher and W. Kurz, *Fundamentals of Solidification*, 3rd ed. Trans Tech Publications, Switzerland, 1998, p 316
117. X. Lin, T.M. Yue, H.O. Yang and W.D. Huang, Solidification Behavior and the Evolution of Phase in Laser Rapid Forming of Graded Ti6Al4V-Rene88DT Alloy, *Metall. Mater. Trans. A*, 2007, **38**(1), p 127–137. https://doi.org/10.1007/s11661-006-9021-5
118. X.J. Xu, X. Lin, J. Chen, F. He and W.D. Huang, Laser Rapid Forming of Ti-Ni Functionally Graded Alloy, *Mater. Sci. Forum*, 2007, **561–565**, p 227–230.
119. M.H. Elahinia, M. Hashemi, M. Tabesh and S.B. Bhaduri, Manufacturing and Processing of NiTi Implants: A Review, *Prog. Mater. Sci.*, 2012, **57**(5), p 911–946. https://doi.org/10.1016/j.pmatsci.2011.11.001
120. T.E. Abioye, P.K. Farayibi, P. Kinnel and A.T. Clare, Functionally Graded Ni-Ti Microstructures Synthesised in Process by Direct Laser Metal Deposition, *Int. J. Adv. Manuf. Technol.*, 2015, **79**(5–8), p 843–850. https://doi.org/10.1007/s00170-015-6878-8
121. Y. Chen, L. Fenggui, K. Zhang, P. Nie, S.R.E. Hosseini, K. Feng and Z. Li, Dendritic Microstructure and Hot Cracking of Laser Additive Manufactured Inconel 718 under Improved Base Cooling, *J. Alloys Compd.*, 2016, **670**, p 312–321. https://doi.org/10.1016/j.jallcom.2016.01.250
122. P. Kontis, E. Chauvet, Z. Peng, J. He, A.K. da Silva, D. Raabe, C. Tassin, J.J. Blandin, S. Abed, R. Dendievel, B. Gault and G. Martin, Atomic-Scale Grain Boundary Engineering to Overcome Hot-Cracking in Additively-Manufactured Superalloys, *Acta Mater.*, 2019, **177**, p 209–221.
123. C. Shang, C. Wang, C. Li, G. Yang, G. Xu and J. You, Eliminating the Crack of laser 3D Printed Functionally Graded Material from TA15 to

Inconel718 by Base Preheating, *Opt. Laser Technol.*, 2020, **126**, p 106100. https://doi.org/10.1016/j.optlastec.2020.106100

124. T.L. Murashkina, M.S. Syrtanov and R.S. Laptev, Structural Changes in C36 laves Phase Intermetallic Compound TiCr 2 During Hydrogenation-Dehydrogenation Process, *Russ. Phys. J.*, 2019, **61**(10), p 1940–1946.
125. A.K. Patel, B. Tougas, P. Sharma and J. Huot, Effect of Cooling Rate on the Microstructure and Hydrogen Storage Properties of TiFe with 4 Wt% Zr as an Additive, *J. Mater. Res. Technol.*, 2019, **8**(6), p 5623–5630. https://doi.org/10.1016/j.jmrt.2019.09.030
126. L.D. Bobbio, R.A. Otis, J.P. Borgonia, R.P. Dillon, A.A. Shapiro, Z.K. Liu and A.M. Beese, Additive Manufacturing of a Functionally Graded Material from Ti-6Al-4V to Invar: Experimental Characterization and Thermodynamic Calculations, *Acta Mater.*, 2017, **127**, p 133–142.
127. J. De Keyzer, G. Cacciamani, N. Dupin and P. Wollants, Thermodynamic Modeling and Optimization of the Fe-Ni-Ti System, *Calphad Comput. Coupling Ph. Diag. Thermochem.*, 2009, **33**(1), p 109–123. https://doi.org/10.1016/j.calphad.2008.10.003
128. B.E. Carroll, T.A. Palmer and A.M. Beese, Anisotropic Tensile Behavior of Ti-6Al-4V Components Fabricated with Directed Energy Deposition Additive Manufacturing, *Acta Mater.*, 2015, **87**, p 309–320. https://doi.org/10.1016/j.actamat.2014.12.054
129. S.M. Kelly and S.L. Kampe, Microstructural Evolution in Laser-Deposited Multilayer Ti-6Al-4V Builds: Part II. Thermal Modeling, *Metall. Mater. Trans. A*, 2004, **35**(6), p 1869–1879. https://doi.org/10.1007/s11661-004-0095-7
130. M. Ghosh, S. Chatterjee and B. Mishra, The Effect of Intermetallics on the Strength Properties of Diffusion Bonds Formed Between Ti–5.5Al–2.4V and 304 Stainless Steel, *Mater. Sci. Eng. A*, 2003, **363**(1–2), p 268–274. https://doi.org/10.1016/S0921-5093(03)00649-X
131. M. Ghosh and S. Chatterjee, Diffusion Bonded Transition Joints of Titanium to Stainless Steel with Improved Properties, *Mater. Sci. Eng. A*, 2003, **358**(1–2), p 152–158.
132. J.M. Wilson and Y.C. Shin, Microstructure and Wear Properties of Laser-Deposited Functionally Graded Inconel 690 Reinforced with TiC, *Surf. Coat. Technol.*, 2012, **207**, p 517–522. https://doi.org/10.1016/j.surfcoat.2012.07.058
133. W.J. Sames, F.A. List, S. Pannala, R.R. Dehoff and S.S. Babu, The Metallurgy and Processing Science of Metal Additive Manufacturing, *Int. Mater. Rev.*, 2016, **61**(5), p 315–360. https://doi.org/10.1080/09506608.2015.1116649